Differential effect of amyloid beta peptides on mitochondrial axonal trafficking depends on their state of aggregation and binding to the plasma membrane

Liang Zhang[a], **Sergey Trushin**[a], **Trace A. Christensen**[b], **Utkarsh Tripathi**[a], **Courtney Hong**[a], **Rachel E. Geroux**[a], **Kyle G. Howell**[a,b], **Joseph F. Poduslo**[a,c], **Eugenia Trushina**[a,d,*]

Liang Zhang: Zhang.liang@mayo.edu; Sergey Trushin: Trushin.Sergey@mayo.edu; Trace A. Christensen: Christensen.Trace@mayo.edu; Utkarsh Tripathi: Tripathi.Utkarsh@mayo.edu; Rachel E. Geroux: Geroux.Rachel@mayo.edu; Kyle G. Howell: Howell.kyle@mayo.edu; Joseph F. Poduslo: poduslo@mayo.edu; Eugenia Trushina: Trushina.eugenia@mayo.edu

[a]Department of Neurology, Mayo Clinic, 200 First St. SW, Rochester, MN 55905, USA

[b]Microscopy and Cell Analysis Core Facility, Mayo Clinic, 200 First St. SW, Rochester, MN, 55905, USA

[c]Department of Biochemistry and Molecular Biology, Mayo Clinic, 200 First St. SW, Rochester, MN 55905, USA

[d]Department of Molecular Pharmacology and Experimental Therapeutics, Mayo Clinic, 200 First St. SW, Rochester, MN 55905, USA

Abstract

Inhibition of mitochondrial axonal trafficking by amyloid beta (Aβ) peptides has been implicated in early pathophysiology of Alzheimer's Disease (AD). Yet, it remains unclear whether the loss of motility inevitably induces the loss of mitochondrial function, and whether restoration of axonal trafficking represents a valid therapeutic target. Moreover, while some investigations identify Aβ oligomers as the culprit of trafficking inhibition, others propose that fibrils play the detrimental role. We have examined the effect of a panel of Aβ peptides with different mutations found in familial AD on mitochondrial motility in primary cortical mouse neurons. Peptides with higher propensity to aggregate inhibit mitochondrial trafficking to a greater extent with fibrils inducing the strongest inhibition. Binding of Aβ peptides to the plasma membrane was sufficient to induce trafficking inhibition where peptides with reduced plasma membrane binding and internalization had lesser effect on mitochondrial motility. We also found that Aβ peptide with Icelandic mutation A673T affects axonal trafficking of mitochondria but has very low rates of plasma membrane binding and internalization in neurons, which could explain its relatively low toxicity. Inhibition of mitochondrial dynamics caused by Aβ peptides or fibrils did not instantly affect mitochondrial bioenergetic and function. Our results support a mechanism where inhibition of axonal trafficking is initiated at the plasma membrane by soluble low molecular weight Aβ species and is exacerbated by fibrils. Since trafficking inhibition does not coincide with the loss

*Corresponding author at: 200 First Street SW, Mayo Clinic, Guggenheim Bld., Room 1542B, Rochester, MN 55905, USA.

Conflict of interest

The authors declare no competing financial interests.

of mitochondrial function, restoration of axonal transport could be beneficial at early stages of AD progression. However, strategies designed to block Aβ aggregation or fibril formation alone without ensuring the efficient clearance of soluble Aβ may not be sufficient to alleviate the trafficking phenotype.

Keywords

Alzheimer's disease; Amyloid beta peptides; Mitochondria; Oligomers; Atomic force microscopy; Dynamic light scattering; Fibrils; Axonal transport; Endocytosis; Mitochondrial function; Bioenergetics; Electron microscopy; Seahorse extracellular flux analyzer; Mouse models of AD; Primary neurons; Plasma membrane binding; Aggregation

1. Introduction

Alzheimer's Disease (AD) is a progressive neurodegenerative disorder that involves loss of memory and cognitive abilities. AD presently affects > 5 million Americans with numbers expected to grow (Alzheimer's Association, 2017). Extracellular neuritic plaques that contain amyloid β (Aβ) aggregated peptides and intracellular neurofibrillary tangles consisting of hyperphosphorylated microtubule-associated Tau protein are two major hallmarks of AD (Bossy-Wetzel et al., 2004; Selkoe, 2003). The key role for Aβ peptides in the pathophysiology of AD was suggested based on the evidence that mutations in the genes that encode amyloid precursor protein (APP) and presenilin 1 and 2 (PS1 and PS2) found in patients with the early-onset familial AD (FAD) lead to significant accumulation of these peptides in the brain (Querfurth and LaFerla, 2010). APP is a membrane-spanning glycoprotein, which is present at the plasma membrane, endoplasmic reticulum (ER), trans-Golgi network (TGN) and endocytic vesicles (Canevari et al., 2004). APP processing is complex where three different enzymes rapidly metabolize it producing either toxic or non-toxic Aβ fragments (O'Brien and Wong, 2011). Most of the APP cleavage occurs at the cell surface, where it is delivered from the TGN in clathrin-coated vesicles, or inside the cell at the TGN and the ER. At the plasma membrane, α-secretase cleaves APP inside the Aβ region producing extracellular, soluble peptides that are not neurotoxic. However, if APP gets re-internalized in endosomal compartments containing β-secretase (β-APP cleaving enzyme, BACE1) and γ-secretase, cleavage produces amyloidogenic, toxic peptides with 40 and 42 amino acids. These peptides are secreted in the extracellular space in association with exosomes, intraluminal vesicles or multivesicular bodies (MVBs) during their fusion with the plasma membrane (Rajendran et al., 2006). The mechanism behind this preferential cleavage of the APP by one of the secretases is not well characterized but has been linked to the lateral organization of membranes and the particular compartmentalization of different proteases in lipid rafts (Ehehalt et al., 2003). Along with the extracellular pool of secreted Aβ, high levels of Aβ peptides are detected inside neurons. Intracellular accumulation of Aβ is attributed to the APP processing by the BACE1 at the TGN and the ER (Greenfield et al., 1999; LaFerla et al., 2007). Moreover, extracellular Aβ peptides secreted at a high concentration by astrocytes could be internalized in neurons via endocytosis contributing to the intracellular Aβ pool (Busciglio et al., 1993; Kandimalla et al., 2009). Depending on the length and the peptide origin, extracellular Aβ peptides could form fibrils and

amyloid plaques. The fibrillization model suggests that native proteins misfold and undergo conformational changes. When these misfolded proteins reach a critical concentration, oligomers are formed that result in protofibrils, and finally culminate in mature fibrils. Furthermore, mature fibrils catalyze the secondary nucleation reaction by forming diffusible oligomers from the monomers (Benseny-Cases et al., 2012; Cohen et al., 2013). Thus, at any given time, the neuron could be exposed to a variety of intracellular and extracellular Aβ species that range from monomers to oligomers and fibrils.

One of the well-characterized cellular targets of pathological Aβ peptides is mitochondrion. Altered energy production and increased generation of reactive oxygen species (ROS) is well documented in AD (Tonnies and Trushina, 2017). Interestingly, while the presence of Aβ plaques is essential for AD diagnosis, Aβ peptides may not be a primary cause of neurodegeneration (Jack Jr et al., 2014). There is compelling data suggesting that increased levels of Aβ may be a consequence of the upstream pathological mechanisms that could directly or indirectly affect APP processing and the generation of toxic Aβ species (Area-Gomez and Schon, 2017; Kepp, 2017; Swerdlow et al., 2014). Some of these mechanisms may include mitochondrial dysfunction associated with aging, the exposure to environmental toxicants, or genetic variations in mitochondrial haplotype. Increased production of ROS by dysfunctional mitochondria could activate pathological cascade of events known as a "vicious cycle" inducing greater severity of metabolic and epigenetic alterations. This, in turn, could affect multiple essential neuronal functions including an abnormal APP processing and the generation of toxic Aβ peptides, ultimately leading to the loss of cognitive function (Pimplikar et al., 2010; Swerdlow et al., 2014; Tonnies and Trushina, 2017; Yu et al., 2016). Moreover, once produced, Aβ peptides could exacerbate mitochondrial dysfunction by incorporating into the organelle and affecting their protein import and ATP production, further enhancing generation of ROS and Aβ (Chen and Yan, 2010; Hansson Petersen et al., 2008a; Mossmann et al., 2014). This novel approach to the understanding of the etiology of late onset sporadic AD, the most prevalent form of the disease, is known as a mitochondrial cascade hypothesis, which views mitochondrial dysfunction as a trigger of the amyloid cascade (Swerdlow et al., 2014).

The fidelity of mitochondrial function in neurons depends on multiple factors. One of the essential components of normal mitochondrial dynamics is the ability to move along axons delivering energy to the distal sites, synapses, and axonal growth cone (Sheng and Cai, 2012). Axonal trafficking is also essential for delivering damaged mitochondria to the soma for degradation (Lin et al., 2017). Mounting data generated in tissue and cells from AD patients and in animal models of FAD suggest mitochondrial axonal trafficking is affected early in the disease prior to the onset of memory impairment or the development of amyloid plaques (Correia et al., 2016; Galindo et al., 2010; Pigino et al., 2003; Selfridge et al., 2013; Tillement et al., 2011; Trushina et al., 2012; Yao et al., 2009; Ye et al., 2012). We have previously demonstrated that bidirectional inhibition of mitochondrial trafficking was already observed in embryonic neurons from different mouse models with familial AD mutations prior to the formation of aggregated endogenous Aβ peptides (Trushina et al., 2012). Since mitochondrial motility plays an essential role in supporting synaptic activity and calcium buffering (Hollenbeck, 1996; Hollenbeck and Saxton, 2005; Mar et al., 2014), alterations in mitochondrial dynamics could contribute to synaptic dysfunction, neuronal

loss and memory deterioration (Calkins and Reddy, 2011). However, it remains unclear to what extent various Aβ species affect axonal trafficking based on their localization (intracellular vs. extracellular), sequence or aggregation state.

A direct impact of Aβ peptides on mitochondrial motility with respect to the state of Aβ aggregation has been investigated in a number of cellular and animal models (Calkins et al., 2011; Calkins and Reddy, 2011; Chen and Chan, 2009; Decker et al., 2010; Iijima-Ando et al., 2009; Rui et al., 2010; Rui et al., 2006; Rui and Zheng, 2016; Trushina et al., 2012; Wang et al., 2010). However, while some studies demonstrated that axonal trafficking is mostly affected by soluble Aβ oligomers, others suggest that fibrils are the most detrimental species (Decker et al., 2010; Meyer-Luehmann et al., 2008; Pigino et al., 2009; Poon et al., 2011; Poon et al., 2013; Ramser et al., 2013; Wang et al., 2010). Moreover, different methods adopted by individual laboratories for Aβ peptide preparation, significant range of doses utilized in the experiments, the duration of treatment, and the variety of cellular models and methods to monitor axonal motility make a direct comparison and the result interpretation difficult. Additionally, precise characterization and quantification of Aβ species is technically challenging further complicating the interpretation of these studies (Benilova et al., 2012). Most often, *in vitro* studies were conducted with pathogenic Aβ40 and/or Aβ42 peptides that are found in brain tissue of AD patients (Swomley et al., 2014). However, there are several mutations in the N- or C-terminus, and in the Aβ region of APP that are associated with FAD. All of these mutations promote the accumulation of toxic Aβ40 and Aβ42 peptides, the increase of Aβ42/Aβ40 ratio, the propensity of these peptides to aggregate, or specifically increase a production of toxic oligomeric species (Hatami et al., 2017). For example, the Osaka (E22Δ) mutation accelerates Aβ aggregation without affecting total Aβ levels while the Italian (E22K) and Arctic (E22G) mutations induce a formation of stable oligomers and protofibrils (Jonsson et al., 2012; Masuda et al., 2008; Nilsberth et al., 2001; Ovchinnikova et al., 2011; Tomiyama et al., 2008). In contrast, a coding mutation (A673T) in the APP gene identified in the Icelandic population was linked to a protection against AD and cognitive decline in dementia-free elderly individuals (Jonsson et al., 2012). This amino acid substitution is located near the aspartyl protease β-site in APP and results in an approximately 40% reduction in the formation of amyloidogenic peptides in vitro (Kokawa et al., 2015; Maloney et al., 2014). The protective effect, therefore, was attributed to the low levels of peptide formation supporting the hypothesis that reducing the β-cleavage of APP may protect against the disease (Jonsson et al., 2012). However, no additional investigation of the effect of this peptide on mitochondria trafficking and function in neurons has been conducted. The objective of our study was to compare side by side the effect of multiple Aβ peptides on mitochondrial motility in live neurons, and to comprehensively characterize the relationship between the peptide structures in dynamic relationship to the effect on axonal trafficking using variety of biochemical techniques. Thus, along with the conventional Aβ40 and Aβ42 peptides, we utilized peptides with recently identified familial AD mutation that promotes rapid formation of aggregates (Aβ39E22Δ) (Poduslo et al., 2012; Tomiyama et al., 2008) and the protective peptide that was found in the Icelandic population (Aβ40A2T) (Jonsson et al., 2012). We also used a peptide previously characterized in our laboratory with mutation that significantly reduces plasma membrane binding and internalization in neurons (Aβ40H13G) (Poduslo et al.,

2010). We have utilized well-established protocols in order to obtain the same peptides either in soluble monomeric or oligomeric form or as fibrils (Poduslo et al., 2012; Verpillot et al., 2008), and examined the consequences of acute treatment on mitochondrial dynamics. We also assessed whether inhibition of axonal trafficking induces mitochondrial dysfunction by monitoring major parameters of mitochondrial energetics in neurons treated with Aβ peptides using a Seahorse Extracellular Flux Analyzer.

We report here that soluble Aβ peptides with high propensity to aggregate have larger effect on trafficking inhibition with fibrils affecting mitochondrial motility most strongly. We also conclude that exogenous Aβ peptides initiate signaling cascade involved in the axonal trafficking inhibition at the plasma membrane. Binding to the neuronal plasma membrane is sufficient to cause rapid and significant inhibition of axonal transport. We found that the lesser effect of Icelandic Aβ peptide on axonal transport compared to Aβ40 and Aβ42 peptides could be attributed to its significantly decreased rate of binding and internalization in neurons. Finally, our data suggest that there is a spatial separation between trafficking inhibition and a loss of mitochondrial function suggesting that therapeutic strategies aimed to improve axonal trafficking early in the disease progression could be beneficial.

2. Material and methods

2.1. Animals

Animal care and handling procedures were approved by the Mayo Clinical Institutional Animal Care and Use Committee in accordance with the National Institutes of Health's Guide for the Care and Use of Laboratory Animals. The following mice were used in the study: a double cross between APP$_{SWE}$ (K670N, M671L) (Hsiao et al., 1996) and PS1 (M146L) (Duff et al., 1996) to produce a double transgenic APP/ PS1 mice (Holcomb et al., 1998). Genotypes were determined by PCR as described in (Trushina et al., 2012). Time-pregnant (E17) wild-type C57BL/6 mice were used for neuronal cultures.

2.2. Neuronal cultures

Preparation and culture of primary embryonic (E17) cortical neurons from wild-type C57BL/6 mice was performed as described previously (Trushina et al., 2003; Trushina et al., 2012). All experiments were done in neurons cultured for 7 days unless specifically stated.

2.3. Aβ peptides

Human Aβ peptides utilized in the study (Table 1) were synthesized on a CEM Liberty (Mathews, NC) peptide synthesizer using HBTU activation and the manufacturer's suggested synthesis protocols. The starting resin was Val-NovaSyn TGA (Novabiochem EMD Biosciences, San Diego, CA). The peptides were then cleaved from the resin support using 5% crystalline phenol, 5% water, 2.5% triisopropylsilane, and 87.5% TFA for 2 h at RT. Each peptide was purified by reverse-phase HPLC on a Jupiter C18 column (250 mm × 21.2 mm, Phenomenex Corp) using a gradient system of 0.1% aqueous TFA containing 80% acetonitrile/water/0.1% TFA. The calculated mass weight was 4329 amu for Aβ40; 4249 amu for Aβ40H13G; and 4514 amu for Aβ42; 4200 amu for Aβ39E22 ,

and 4359 amu for Aβ40A2T as confirmed by electrospray ionization mass spectrometry (Thermoelectron Surveyor MSQ). Peptide sequences were as following: Aβ1-40 (Aβ40): DAEFR-HDSGYEVHHQKLVFFAEDVGSNKGAIIGLMVGGVV; Aβ1-40H13G (Aβ-40H13G): DAEFRHDSGYEVGHQKLVFFAEDVGSNKGAIIGLMVGGVV; Aβ1-42 (Aβ42): DAEFRHDSGYEVHHQKLVFFAEDVGSNKGAIIGLMVG-GVVIA; Aβ39E22 : DAEFRHDSGYEVHHQKLVFFADVGSNKGAIIGLM-VGGVV; and Aβ40A2T: DTEFRHDSGYEVHHQKLVFFAEDVGSNKGAII-GLMVGGVV. Fluorescein-conjugated F-Aβ40, F-Aβ40H13G, and FAβ40A2T peptides were synthesized with Ahx (Fmoc-6-amino hexanoic acid) attached to the N-terminal for subsequent coupling with flkuor-escein as previously described (Poduslo et al., 2010). Molecular weights of peptides were as following: F-Aβ40 4801 amu;β40H13G F-A 4721 amu; and F-Aβ40A2T 4831 amu.

2.4. Preparation of soluble Aβ peptides

Dissolution medium and storage conditions are critical parameters for amyloid peptides that are prone to aggregation or fibrillogenesis. To ensure the presence of predominantly monomeric form in the starting solutions, all peptide samples, which were received in lyophilized form, were individually dissolved in aqueous solution of 0.40% ammonium hydroxide (Verpillot et al., 2008). These solutions were then divided into several aliquots and individually stored at −20 °C. Each aliquot was thawed only once immediately prior to the experiment; aliquots were never refrozen. Peptide solutions for atomic force microscopy (AFM) or electron microscopy (EM) were prepared by adding 0.01 M sodium phosphate buffer (pH 7.4) to achieve the final peptide concentration of 100 or 0.1 μM, respectively. All peptides used in the axonal trafficking assay, TEM, AFM and bioenergetic studies were sonicated prior to the addition to the cells.

2.5. Preparation of fibrillar Aβ peptides

Peptides were solubilized in 0.01 M sodium phosphate buffer (pH 7.4) containing 0.01% (w/v) NaN_3 so that the final concentration was 100 μM. Peptides were incubated for 7 days at 37 °C using an Innova 40 incubator shaker (New Brunswick). The same peptide samples from the 96-well plate were pooled in a 1.5 ml microcentrifuge tube (Fisher Scientific). Fibril formation was confirmed using EM (concentration 100 μM) and AFM. For AFM, fibrils were diluted to the concentration 1 or 0.1 μM in 0.01 M sodium phosphate buffer (pH 7.4) and observed without sonication. Fibrils were diluted into cell culture medium (1–4 μM) for axonal trafficking assay or bioenergetic assay without prior sonication.

2.6. Western blot analysis

Aβ peptides (0.9–1 μg/μl) prepared using ammonium hydroxide were separated using 4–15% Tris-HCl Gradient Gel (BioRad) using Tris/ Glycine/SDS-containing running buffer. Primary antibodies were 6E10 (mouse monoclonal, 1:3000 dilution, BioLegend, CA) and 4G8 (mouse monoclonal, 1:10,000 dilution, BioLegend, CA). Secondary antibody was α-Mu (1:15,000 dilution, BioLegend, CA).

2.7. Treatment with Aβ peptides and time-lapse imaging of axonal trafficking in neurons

Primary embryonic cortical neurons (E17) from time-pregnant C57Bl/6 mice were plated and cultured for 7 days. Peptides were directly dissolved in the culture medium to the desired concentration (1–4 μM); cells were incubated for 30 min, and the analysis of axonal trafficking was performed using time-lapse imaging as described previously (Trushina et al., 2004; Trushina et al., 2012; Zhang et al., 2016b; Zhang et al., 2015). Briefly, mitochondria in control neurons and neurons treated with Aβ peptides were visualized using Mitotracker Orange CMTMRos or tetramethylrhodamine, methyl ester (TMRM) (Molecular Probes, Eugene, OR) (final concentration 50 nM, 15 min incubation). TMRM is a membrane-potential-sensitive, cationic fluorophore that incorporates into actively respiring mitochondria. Thus, TMRM allows detecting the motility of functioning mitochondria and the effect of treatment on membrane potential. In our previous studies, we determined that none of these dyes affect axonal trafficking of mitochondria under experimental paradigm utilized in our experiments compared to the rates of axonal trafficking determined in neurons using Nomarski optics (no dye added) (Trushina et al., 2004). Mitotracker and Aβ peptides were added directly to cells without prior washing. After 15 min of incubation, the medium was replaced with fresh F-12K (phenol red-free) medium (37 °C) following with time-lapse imaging. Experiments were performed using confocal Laser Scanning Microscope (LSM 510, Carl Zeiss Inc., Germany) with a Plan-Apochromat 100× (1.4 n.a.) oil objective. Cells were incubated at 37 °C during the time of recording. All recordings were started 5 min after the coverslip was placed on the microscopic stage to allow equilibration of the sample. Laser was set up to 543 nm for excitation; emission was collected at 585 nm and greater. Laser power was kept below 4%; the pinhole was completely open. Under these conditions, we did not observe any photobleaching through the entire time of recording. Assay validation determined that three individual neurons could be reliably and reproducibly assayed from one coverslip. Axons were selected based on the lack of branching through the entire length, and the uniform region that immediately follows the hillock was positioned across the window of observation to get the most mitochondria movement per length. A total of 600 frames were recorded per cell. Images were taken every 1 s at highest scan speed (0.9 s) for 10 min. Three different cells were imaged from each coverslip; exactly the same experimental conditions were maintained from experiment to experiment to allow a direct comparison. Movies were analyzed using LSM 510 software that allowed animation of 600 images into a "movie". For analysis of axonal trafficking, each mitochondrion was traced from the first frame of the movie to the last. We recorded time and distance that a particular organelle traveled in axon, and calculated velocities in anterograde (from the cell body) and retrograde (to the cell body) directions (Trushina et al., 2004). We also measured the length of each organelle at the beginning of the imaging. At least 15 neurons from 3 to 5 independent cultures were analyzed for each experiment. 35–70 individual organelles were taken into the analysis for each condition. Kymographs were generated using ImageJ software.

2.8. IgG4.1 treatment

Cortical neurons 7 DIC were pretreated with 0, 1, 2 and 4 μM of IgG4.1 antibody for 30 min followed by the addition of 0, 2 or 4 μM of Aβ42 for additional 30 min. IgG4.1 is a monoclonal antibody directed against fibrillar human Aβ42, which recognizes N-terminal

residues 2–11 (Poduslo et al., 2007; Ramakrishnan et al., 2009; Ramakrishnan et al., 2008). Axonal trafficking was examined using Mitotracker Orange CMTMRos and time-lapse imaging as described above.

2.9. Transmission electron microscopy (TEM)

Peptides originally dissolved in NH_4OH or fibrils prepared without NH_4OH were diluted in 0.01 M sodium phosphate buffer (pH 7.4) containing 0.01% (w/v) NaN_3 to the final peptide concentration of 100 μM. Carbon-coated Formvar 300 mesh copper grids (Electron Microscopy Sciences, Hatfield, PA) were spotted with 3 μl of peptide sample and allowed to stand for 1 min. The solution was wicked away with filter paper, and the peptide was rinsed twice with 3 μl of nanopure water. The negative stain was performed using 3 μl of 0.1% uranyl acetate and allowed to sit briefly prior to a removal. Each grid was rinsed twice with 3 μl of nanopure water and allowed to dry. The entire staining process took ~5 min. Grids were air dried and imaged. Micrographs were acquired using JEOL 1400 transmission EM microscope (JEOL Ltd., Tokyo, Japan) at magnifications of 15,000×, 60,000×, and 100,000×.

For conventional TEM in the brain tissue of APP/PS1 mice, animals were perfused with 4% paraformaldehyde, brains were removed and post-fixed in Trump's solution overnight (Trushina et al., 2012). Next day, hippocampal CA1 region was dissected from each brain and subjected to EM staining. CA1 Hippocampal tissue was incubated in 1% osmium tetroxide, dehydrated in a graded series of ethanol and embedded in Quetol 651 (Ted Pella, Inc.). Thin sections (0.09–0.1 μm) were cut parallel to the ventral surface using a diamond knife (Diatome US) and an Ultracut E microtome (Reichert-Jung, Wien, Austria). Sections were collected on copper grids, post-stained with lead citrate and viewed at ~80 kV with a JEOL 1400 transmission electron microscope (JEOL USA). Ten randomly selected plaque-containing micrographs per mouse were analyzed. The following mice were used for the EM examination: three APP/PS1 female mice 6 months of age and three APP/ PS1 female mice 22 months of age.

2.10. Atomic force microscopy (AFM)

Soluble and fibrillar peptides prepared as described above were solubilized in 0.01 M sodium phosphate buffer (pH 7.4) containing 0.01% (w/v) NaN_3 to a concentration of 0.1–4 μM. Immediately, 10 μl of a sample was added to a freshly cleaved layer of mica (Ted Pella, Inc., Redding, CA.) and allowed to air dry. AFM measurements were carried out on dry peptide samples with silicon nitride NP-S20 tips (Veeco Metrology, Inc., Santa Barbara, CA) using a MultiMode Scanning Probe Microscope (MM SPM) with a NanoScope IV controller. A high resolution J-type scanner was used to scan the peptide surface. Images were collected by raster scanning across a 10 $μm^2$ area at 1024 samples (pixels) per line at a rate of 3.70 Hz. Images were processed with NanoScope Software (Veeco Metrology, Inc.).

2.11. Dynamic light scattering

Dynamic light scattering was performed with Aβ peptides prepared using NH_4OH. Peptides were diluted to the final concentration of 100 or 5 μM in double distilled water, and

placed into the Zetasizer nano series instrument (Malvern) for observation. Scanning was performed every 5 min for the total of 30 min.

2.12. Internalization assay

Fluorescein-conjugated F-Aβ40, F-Aβ40H13G, and F-Aβ40A2T peptides (2 μM) were prepared using NH_4OH as described above. Cortical neurons plated on poly-L-ornithine-coated glass cover slips were washed with HEPES-buffered MEM (10 mM HMEM) at room temperature and then incubated with Aβ peptides for 10 min at 37 °C in the incubator with 5% CO_2 to induce endocytosis. Excess of fluorescent peptides at the cell surface was removed by acid stripping (Trushina et al., 2006). After incubation, the medium was replaced with ice-cold HMEM without glucose, and the culture dishes were transferred to a 10 °C bath. Cells were observed using LSM 780 confocal microscope (Carl Zeiss Inc., Germany) with a Plan-Apochromat 100× (1.4 n.a.) oil objective. 30 cells from each experiment were taken into the analysis. Experiments were repeated three times. In some experiments, TMRM was added to visualize mitochondria and their colocalization with Aβ peptides in live neurons.

2.13. Mitochondrial respiration

Primary embryonic cortical neurons (E17) from Bl6 mice were seeded in the 24 well plates (Seahorse Biosciences, North Billerica, MA) covered with poly-L-ornithine at 1×10^5 cells per well and cultured for 6–7 days in Neurobasal media (Zhang and Trushina, 2017). Cells were treated with vehicle, 2 μM of soluble Aβ40, Aβ42, Aβ40H13G, and Aβ40A2T prepared using NH_4OH or 2 μM of Aβ40, Aβ42, and Aβ40H13G 7-day fibrils dissolved in fresh bicarbonate-free DMEM containing 25 mM glucose, 0.5 mM glutamine and 0.2 mM pyruvate for 30 min at 37 °C and 5% CO_2. Formation of fibrils prior to the addition to cells was confirmed using TEM. Before subjecting cells to mitochondria stress test, cells were washed once with fresh media. Oxygen Consumption Rate (OCR) was assessed using a Seahorse XF24 Extracellular Flux Analyzer (Seahorse Biosciences, North Billerica, MA). Baseline OCR was assessed with 3 measurement loops consisting of a 3 min mix cycle, a 2 min delay cycle, and a 3 min measurement cycle. Respiratory chain inhibitors were sequentially injected into the wells as described in (Lange et al., 2012; Zhang and Trushina, 2017). Briefly, the ATP-coupled OCR was calculated as the fraction of the basal OCR sensitive to 1 μg/ml of an ATP synthase inhibitor oligomycin. Maximal uncoupled respiration rate was determined by depolarizing mitochondrial membrane potential with 0.75 μM carbonyl cyanide-p-trifluoromethoxyphenylhydrazone (FCCP). Non-mitochondrial respiration was determined as the activity remaining after inhibition of complexes I and III with 0.75 μM rotenone and 0.75 μM antimycin A, respectively. At the end of the experiments, cells were harvested, and protein content of each well was determined using Bradford assay. Mitochondrial respiration values were normalized to protein content of each well. Mitochondrial coupling efficiency was determined as a ratio between ATP turnover and basal respiration. Maximum respiratory capacity, spare respiratory capacity and respiratory state apparent (State$_{app}$) were determined as described in (Brand and Nicholls, 2011; Sansbury et al., 2011).

2.14. Statistical analysis

Unless specifically mentioned, data were analyzed using Student t-test. $P < 0.05$ was considered statistically significant.

3. Results

3.1. Soluble Aβ42 peptides with higher propensity to aggregate affect mitochondrial trafficking to a greater extent compared to Aβ40 peptides

Aβ peptides tend to form multiple species in the solution spanning from monomers to oligomers to protofibrils (Tsigelny et al., 2014). To examine the effect on axonal trafficking in neurons, Aβ40 and Aβ42 peptides were prepared using ammonium hydroxide that reportedly should maintain peptides primarily in monomeric soluble form (Verpillot et al., 2008). To ensure that both peptides added to neurons were in the soluble monomeric form, we examined the composition of each peptide in the solution starting immediately after the preparation and for the next 30 min using dynamic light scattering (Fig. 1a). We have found differences in peptide behavior. Peak corresponding to the monomeric Aβ40 was present in the solution for the first 10 min after the preparation with peaks corresponding to the high molecular weight soluble Aβ40 species appearing later (Fig. 1a, upper panel, asterisk denotes monomeric Aβ40). In contrast, we did not detect the monomeric Aβ42 peak at any time of observation. Immediately after the preparation, solution of Aβ42 contained high molecular weight soluble oligomers (Fig. 1a, bottom panel). Similar results indicating higher propensity of Aβ42 to form oligomers immediately after the dissolving were obtained after the examination of peptides within 5 min after the preparation using atomic force microscopy (AFM) (Fig. 1b). While Aβ40 peptides were detected primarily in the monomeric form (Fig. 1b, top panel), Aβ42 peptides formed a mixture of oligomers (Fig. 1b, bottom panel). These observations were also confirmed using western blot analysis (Fig. 1c, Aβ40 and Aβ42). Thus, in freshly prepared solutions, Aβ42 peptides rapidly form high molecular weight oligomers while Aβ40 peptides stay as monomers for at least 10 min after the preparation.

We next examined the effect of Aβ40 and Aβ42 peptides prepared using ammonium hydroxide on axonal trafficking of mitochondria in live primary embryonic (E17) cortical neurons from wild-type mice using time-lapse imaging assay developed in our laboratory (Trushina et al., 2004; Trushina et al., 2012; Zhang et al., 2015). Mitochondria were visualized using a non-toxic TMRM dye (Fig. 2 a–c), which, as we have shown previously by comparing rates of axonal trafficking in neurons using Nomarski optics, has no effect on mitochondrial motility (Trushina et al., 2004). Mitochondrial movement to (retrograde) and from (anterograde) the cell body was examined in cells treated with different concentrations of Aβ peptides, and compared to untreated cells (Fig. 2d). Concentrations of Aβ peptides (1–4 μM) were selected based on the lack of cell death within 24 h after treatment determined with trypan blue staining (data not shown). We have found that both Aβ40 and Aβ42 peptides significantly inhibit mitochondrial trafficking in anterograde and retrograde directions (Fig. 2d). Data obtained in a large cohort of neurons (20–30 cells per experiment, at least three biological replicates) demonstrate that Aβ42 induced stronger trafficking inhibition in both directions compared to Aβ40. Incubation with 4 μM

of Aβ40 resulted in ~15% reduction of mitochondrial rates in anterograde and ~32% in retrograde direction while treatment with the same concentration of Aβ42 lead to ~42% of trafficking inhibition in both directions (Fig. 2d). It is interesting to note that trafficking inhibition in neurons treated with Aβ40 vs. Aβ42 was not consistently dose-dependent (Fig. 2d). While anterograde trafficking of mitochondria was inhibited in a dose-dependent manner in anterograde direction by Aβ42 peptide and in retrograde direction by Aβ 40 peptide, treatment with 4 μM of Aβ40 actually increased rates of mitochondria motility in anterograde direction. One of the explanation could include the compensatory effect since under these conditions over 80% of mitochondria are already stationary while remaining 20% of organelles have to respond to metabolic demand of the cell (Fig. 2d,e). It is well known that mitochondria display a variety of movement patterns in neurons such as smooth, non-stop motion without a change in the direction; a stop-and-go motion with multiple changes in the direction; a saltatory movement without a net direction, and a large number of mitochondria often remain stationary (Chada and Hollenbeck, 2003; Hollenbeck and Saxton, 2005; Overly et al., 1996; Trushina et al., 2004). In our experiments, ~50% of mitochondria were stationary in control neurons (did not move over 10 min of observation, Fig. 2e). In contrast, in neurons treated with Aβ peptides, the number of stationary mitochondria significantly increased. However, despite a stronger effect of Aβ42 peptides on the rate of mitochondrial trafficking (Fig. 2d), an increase in stationary mitochondria did not differ significantly between Aβ40 and Aβ42 neurons treated with 2 μM of peptides. These changes became significant only at a high concentration where the number of stationary mitochondria reached almost 100% in Aβ42-treated neurons (Fig. 2e). These data may indicate that trafficking inhibition does not immediately result in organelle immobilization. However, at high concentrations of Aβ peptides, trafficking inhibition coincides with organelle immobilization (Fig. 2d,e). Mitochondrial motility in untreated cells (Fig. 2f) and in neurons treated with Aβ peptides (Fig. 2g,h) is illustrated in kymographs generated by combining 600 frames collected over a 10 min time period. An increase in stationary mitochondria and a decrease in moving organelles after Aβ treatment are demonstrated by a significant reduction in diagonal lines representing mitochondrial movement and an increase in parallel lines representing stationary organelles (Fig. 2f–h). These data suggest that both monomeric and oligomeric soluble Aβ species affect axonal trafficking. However, higher propensity of Aβ42 to aggregate may account for a stronger inhibitory effect on mitochondrial motility and immobilization (Fig. 2).

3.2. Aβ peptides with higher propensity to aggregate and Aβ fibrils induce stronger axonal trafficking inhibition compared to soluble Aβ peptides

To examine to what extent aggregated Aβ peptides affect axonal trafficking compared to soluble oligomers, we utilized the recently identified Aβ variant lacking glutamate 22 (Aβ39E22) found in Japanese families with Alzheimer's-type dementia (Tomiyama et al., 2008). This peptide shows enhanced aggregation and rapidly converts to fibrils in solution (Cloe et al., 2011; Poduslo et al., 2012). We first prepared Aβ39E22 using ammonium hydroxide (Fig. 1c, Aβ39E22). In fresh solution, Aβ39E22 rapidly formed oligomers similar to Aβ42 peptide. We next prepared Aβ39E22 and Aβ40 7-day fibrils to examine the effect of the same peptides on axonal trafficking in relationship to their aggregated state (Fig. 3). Formation of Aβ39E22 and Aβ40 fibrils was confirmed with AFM (data

not shown) and TEM (Fig. 3a). Western blot analysis of fibrils in solution confirmed the presence of high molecular weight oligomers and aggregates. We found that soluble Aβ39E22 (Fig. 3b, light green bars) inhibited axonal trafficking to the greater extent than soluble Aβ40 peptide (Fig. 3b, light orange bars). However, both fibrillar Aβ39E22 (Fig. 3b, dark green bars) and fibrillar Aβ40 (Fig. 3b, dark orange bars) induced similar effect on axonal trafficking inhibition, which was stronger compared to soluble Aβ39E22 or Aβ40 peptides. Moreover, fibrillar Aβ40 peptides affected mitochondrial motility to a significantly greater extent compared to soluble Aβ40 peptides (Fig. 3b). For all peptides tested, inhibitory effects were comparable in both anterograde and retrograde directions. Thus, Aβ peptides with high tendency to aggregate inhibit axonal trafficking of mitochondria to a greater extent with fibrils inducing the most significant inhibition compared to soluble oligomers or monomers.

This conclusion was unexpected. Many recent studies provide a compelling support for the notion that soluble oligomeric Aβ peptides represent the most toxic species affecting multiple cellular mechanisms involved in AD including axonal trafficking (Verma et al., 2015). Moreover, formation of fibrils has been proposed to be protective by acting as a reservoir for toxic oligomers (Verma et al., 2015). Therefore, to determine the effect of amyloid aggregates and fibrils on neurons and mitochondria in vivo, we applied TEM to examine the brain tissue in a mouse model of familial AD at two time points corresponding to early and late stages of disease development. This mouse model carries multiple mutations in two human transgenes, APP and PS1, found in familial AD. The mouse model was created by crossbreeding of APP$_{SWE}$ (K670N, M671L) (Hsiao et al., 1996) and PS1 (M146L) (Duff et al., 1996) mice to produce the APP/PS1 mice (Holcomb et al., 1998). These mice express high level of Aβ peptides from birth, and start to develop amyloid plaques around 6 months of age (Holcomb et al., 1998). We examined the CA1 hippocampal brain region of APP/PS1 female mice at 6 and 22 months of age (Fig. 4). We specifically studied areas of the brain in a close proximity to the amyloid plaques at the low (Fig. 4a, b) and high magnification that allowed visualizing individual Aβ fibrils (Fig. 4c, d, F). Our observations revealed that all amyloid plaques observed in the brain tissue of young and old APP/PS1 mice were surrounded by dystrophic neurites (Fig. 4a, b, arrows). Some of these neurites contained mitochondria that could be easily identified (Fig. 4a, b, asterisks). Further examination revealed that in some neurites mitochondria have abnormal cristae organization and morphology indicating mitochondrial dysfunction. However, in other cases, we were able to detect a presence of amyloid fibrils in a close proximity to the plasma membrane of neurites where mitochondria appeared to be normal (Fig. 4c, d, M). These observations support the hypothesis that there is a direct contact between Aβ fibrils and neuronal membranes in vivo that could affect mitochondrial transport and function. Moreover, these interactions could disturb mitochondrial motility early in disease progression and at the later stages of the disease impeding functions of remaining neurons.

3.3. Reduced binding of Aβ peptides to the neuronal plasma membrane rescues trafficking phenotype

We found that axonal trafficking of mitochondria was significantly inhibited within 30 min after the addition of Aβ peptides (Figs. 2d and 3b). Previous observations demonstrated that the molecular mechanisms involved in trafficking inhibition caused by acute exposure to Aβ peptides could involve signaling cascade initiated at the plasma membrane (Mairet-Coello et al., 2013; Rui et al., 2006; Rui and Zheng, 2016). It has also been shown that the accumulation of intracellular Aβ peptides resulting from their endocytosis in neurons occurs early in AD progression prior to the formation of amyloid plaques (Wirths et al., 2004). Within the cell, Aβ could directly bind mitochondria affecting their motility and function (Caspersen et al., 2005; Cha et al., 2012; Hansson Petersen et al., 2008b). We therefore examined to what extent reduced plasma membrane binding and internalization of the extracellular Aβ peptides could rescue trafficking phenotype. Previously, we demonstrated that substitution of the histidine residues of Aβ40, Aβ40H13G, resulted in a dramatic reduction of its binding to neurons (Poduslo et al., 2010; Poduslo et al., 2012). Indeed, treatment of control neurons with soluble Aβ40H13G prepared using ammonium hydroxide (Fig. 1c) had no significant effect on mitochondrial motility in both anterograde and retrograde directions at any concentrations tested (1–4 μM, Fig. 5a) compared to soluble Aβ40 peptide, which significantly inhibited mitochondrial trafficking at concentrations above 1 μM (Fig. 2d). Examination of Aβ40H13G structure in freshly prepared solution using TEM (data not shown) and AFM (Fig. 5b) revealed presence of species in size and appearance similar to the observed in the solution of Aβ40 peptide (Fig. 1a–c). Thus, the lack of the inhibitory effect of Aβ40H13G peptide on axonal trafficking of mitochondria cannot be attributed to the formation of different species but to the significantly reduced plasma membrane binding.

To confirm this finding, we next tested whether the capture of soluble amyloid peptides with a specific monoclonal antibody IgG4.1 known to prevent neuronal binding and internalization of Aβ42 (Poduslo et al., 2007; Ramakrishnan et al., 2009) could also rescue mitochondria trafficking phenotype. Indeed, a pre-treatment with IgG4.1 antibody completely protected neurons from Aβ42 - induced trafficking inhibition in both anterograde and retrograde directions (Fig. 5c). Moreover, neither treatment with Aβ40H13G nor with Aβ42 after the pre-treatment with IgG4.1 antibody resulted in an increase in the amount of stationary mitochondria, which is in a contrast to a significant increase observed in the experiments with Aβ42 alone (Figs. 2e and 5d). These results suggest that binding of the Aβ peptides to the plasma membrane is sufficient to induce axonal trafficking inhibition of mitochondria in neurons.

3.4. Aβ peptide with Icelandic mutation differentially affects axonal trafficking and has reduced rate of internalization in neurons

We next examined the effect of Aβ peptide with A673T substitution (Aβ40A2T) found in the Icelandic population and claimed to be neuroprotective (Jonsson et al., 2012) on axonal trafficking of mitochondria. Cortical neurons were treated with different concentrations of Aβ40A2T prepared using ammonium hydroxide, and axonal trafficking of mitochondria was examined using the same assay as was described for soluble Aβ40 peptide (Figs. 2,

3, 5). We found that in contrast to Aβ40, an acute treatment with Aβ40A2T inhibited rates of mitochondrial motility specifically in retrograde direction (Fig. 6a). Inhibition was dose-dependent, and reached ~25% in cells treated with 4 μM of Aβ40A2T (Fig. 6a) while treatment with the same concentration of Aβ40 inhibited mitochondrial motility by ~50% (Fig. 2d). We extended the analysis to measure distances individual mitochondria traveled between stops in anterograde and retrograde directions, an additional indicator of the integrity of axonal trafficking machinery (Trushina et al., 2004). Treatment with Aβ40A2T peptide differentially affected rates and distances mitochondria traveled in neurons (Fig. 6b). In retrograde direction, treatment with Aβ40A2T resulted in inhibited rates and significantly shortened distances covered by the organelles between stops (Fig. 6b, Retrograde). In contrast, distances coved by mitochondria in anterograde directions significantly increased, most likely representing a compensatory mechanism (Fig. 6b, Anterograde). Similar to Aβ40 peptide, treatment with Aβ40A2T also produced a dose-dependent increase in the amount of stationary organelles (Fig. 6c). Thus, a protective effect βof **40A2T** peptide can't be attributed to the lack of the inhibition of mitochondria motility.

To determine whether A673T substitution in Aβ peptide could affect plasma membrane binding and internalization in neurons, we next examined rates of endocytosis of fluorescently labeled F-Aβ40A2T in live neurons and compared it to F-Aβ40 using our well-established protocol (Trushina et al., 2006). Intracellular levels of F-Aβ40 observed using confocal microscopy 10 min after the addition to neurons were very robust with cells uniformly labeled with green puncta (Fig. 6e, f). F-Aβ40 was also found to colocalize with mitochondria visualized using TMRM (Fig. 6e, top panel). In contrast, internalization of F-Aβ40A2T was significantly reduced compared to F-Aβ40 (Fig. 6e, f). Quantification revealed that the rate of F-Aβ40 internalization was at least 2 fold greater compared to F-Aβ40A2T (Fig. 6d). Similar to F-Aβ40A2T, and as would be expected based on its low plasma membrane binding, we also did not observe any significant internalization of F-Aβ40H13G in neurons (data not shown). These results suggest that significantly lesser effect of Aβ40A2T on axonal trafficking of mitochondria could be associated with reduced plasma membrane binding and endocytosis.

3.5. Acute inhibition of axonal trafficking with Aβ peptides does not affect mitochondrial function

Inhibition of axonal trafficking of mitochondria was observed in multiple cellular and animal models of numerous neurodegenerative diseases including AD, Huntington's (HD) and Parkinson's Diseases (PD) (Beal, 2005; Itoh et al., 2013; Trushina et al., 2004). However, the spatial relationship between inhibition of mitochondrial motility and a loss of function has not been established. It is unclear whether a loss of motility immediately evokes the loss of mitochondrial function or these events are not directly connected. If the latter is true, therapeutic strategies aiming to restore axonal trafficking could be beneficial at early stages of the disease, while at the later stages, combination therapy that targets both the restoration of axonal transport and mitochondrial function should be considered.

To establish whether acute inhibition of axonal dynamics with Aβ peptides induces a loss of mitochondrial function, we compared bioenergetic profiles in live neurons treated

with 2 μM of soluble or fibrillar Aβ40, Aβ42 and Aβ40H13G using a Seahorse XF24
Extracellular Flux Analyzer and mitochondria stress test (Zhang and Trushina, 2017)
(Figs. 7 and 8). Soluble peptides were prepared using ammonium hydroxide and fibrils
were generated over 7 days as described in the Methods. Cell respiration was examined
in a basal state and after the addition of oligomycin (to block ATP synthesis), FCCP
(to uncouple ATP synthesis from the electron transport chain, ETC), and rotenone and
antimycin A (to block complex I and III of the ETC, respectively) (Gerencser et al.,
2009; Nicholls et al., 2010). One of the advantages of using a Seahorse XF24 instrument
is the ability to measure metabolic parameters in intact neurons by monitoring oxygen
consumption rate, an indicator of the oxidative phosphorylation (OXPHOS), in the context
of cellular environment without the need to isolate mitochondria (Figs. 7a, 8a). These major
parameters of mitochondrial respiration include basal oxygen consumption rate (OCR),
spare respiratory capacity (SRC), ATP coupled and uncoupled respiration together with a
non-mitochondrial respiration, proton leak, coupling efficiency, and maximal respiratory
capacity. Measuring these bioenergetic outcomes could inform on the ability of cells to
produce energy under stress conditions and the efficiency of the ETC (Figs. 7 and 8) (Zhang
and Trushina, 2017).

We found that OCR profiles in neurons treated with either soluble or fibrillar Aβ40, Aβ42,
and Aβ40H13G did not differ from profiles of neurons treated with vehicle responding in
an anticipated manner to the addition of all of the mitochondrial stress test reagents (Figs.
7 and 8). Thus, the loss of OCR after the addition of oligomycin; an increase after the
addition of the uncoupler FCCCP; and the decrease after the addition of rotenone/antimycin
A was similar in treated and untreated cells, and did not differ based on the state of peptide
aggregation. Since treatment with 2 μM of Aβ40 or Aβ42 induced a robust inhibition of
mitochondrial transport in neurons (Fig. 2), the bioenergetic data suggest that mitochondrial
function under these conditions was un-affected. Similar, cellular energetics was unaffected
in neurons treated with Aβ40H13G that does not affect axonal transport (Figs. 7 and
8) or Aβ40A2T that affects mitochondrial motility to a lesser extent compared to Aβ40
(data not shown). Furthermore, the addition of oligomycin, FCCP or rotenone/antimycin
A failed to reveal any differences in the rates of SRC, an indicator of the mitochondrial
capacity to produce energy under conditions of increased workload or stress, which is
essential for a long-term neuronal survival and function (Choi et al., 2009; Nicholls et al.,
2010). Similarly, there were no changes in the ATP turnover, maximal respiratory capacity
(MRC), non-mitochondrial respiration or proton leak in treated vs. untreated cells (Figs.
7 and 8). No changes were observed in coupling efficiency or state apparent. These data
indicate that trafficking inhibition induced by acute exposure to Aβ peptides does not
coincide with the loss of mitochondrial function. Our data suggest that there is a window
of therapeutic opportunity where restoration of axonal trafficking could be beneficial to
promote the dynamics of otherwise functional organelles (Figs. 7 and 8). Furthermore, it was
reported that prolonged exposure to Aβ peptides affects mitochondrial length by altering
fission/fusion machinery (Rui and Zheng, 2016). We did not detect significant changes in
mitochondrial length (elongation or fragmentation) 30 min after the addition of various Aβ
peptides to neurons regardless of the peptide origin or state of aggregation (data not shown).
Since mitochondrial fragmentation is associated with mitochondrial dysfunction, this data

support our findings that an acute exposure of neurons to extracellular Aβ peptides primarily affects axonal trafficking and does not cause changes in mitochondrial function.

4. Discussion

We examined the effect of multiple exogenous Aβ peptides in different state of aggregation, soluble vs. fibrillar, on mitochondrial axonal trafficking in primary cortical neurons using an acute treatment (30 min after the peptide addition). Our data suggest that the strongest inhibition of axonal trafficking was observed with Aβ fibrils and peptides with high propensity to aggregate. Another important observation is that binding to the plasma membrane of the external Aβ peptides plays the essential role in trafficking inhibition. Finally, our data demonstrate that acute treatment with Aβ peptides does not alter mitochondrial energetics and the ability to generate energy suggesting a spatial separation between trafficking inhibition and the loss of mitochondrial function.

Inhibition of axonal trafficking of multiple vesicles and organelles, mitochondria in particular is not limited to AD and has been observed early in the progression of multiple neurodegenerative disorders (El-Kadi et al., 2007; Goldstein, 2012; Millecamps and Julien, 2013; Morfini et al., 2009; Palau et al., 2009; Trushina et al., 2004; Trushina et al., 2012). Consequences of axonal trafficking inhibition are linked to altered synaptic transmission, inadequate neurotrophic factor support, altered mitochondrial fission and fusion that eventually leads to the loss of energy production and neuronal death (Calkins et al., 2011; Calkins and Reddy, 2011; Itoh et al., 2013; Reddy et al., 2010; Schwarz, 2013; Yao and Brinton, 2011; Ye et al., 2012). Despite significant research efforts, the underlying molecular mechanism(s) of axonal trafficking inhibition remains unclear. Similar, it remains uncertain whether restoration of axonal trafficking represents a practical therapeutic target for neurodegenerative diseases.

Accumulation of Aβ peptides in the brain tissue is a hallmark of AD. These peptides are produced in brain cells via the enzymatic processing of APP resulting in the pool of intracellular and extracellular Aβ peptides. Depending on the sequence, some peptides rapidly aggregate to form extensive extracellular amyloid plaques. The other, which are primarily soluble, could be cleared from the brain via the interstitial fluid into the cerebrospinal fluid or via a direct trafficking out of the brain past the blood–brain barrier into peripheral circulation (Karran et al., 2011). Thus, a neuron could be exposed to multiple forms of Aβ peptides ranging from monomers and oligomers to protofibrils and fibrils (Tsigelny et al., 2014). Interestingly, various Aβ species distinctively affect cellular functions. Thus, synaptic loss was directly associated with soluble Aβ42 oligomers produced *in vitro* or extracted biochemically from the brains of patients with AD (Jin et al., 2011; Lacor et al., 2004; Shankar et al., 2008). Furthermore, Aβ42 oligomers were shown to induce early synaptotoxic effects and progressive dendritic spine loss by promoting Tau translocation to the dendrites via activation of the CAMKK2-AMPK kinase pathway (Ittner et al., 2010; Miller et al., 2014). The specific effect of amyloid fibrils was associated with the abnormal reorganization of the plasma membrane and aggregation of lipid rafts, which affected GM1 clustering and mobility (Bucciantini et al., 2012; Okada et al., 2008). Remarkably, this effect was not associated with fibril internalization in neurons

but with the initiation of the signaling cascade that involved caspase-8 activation after Fas receptor translocation on fibril binding to the plasma membrane (Bucciantini et al., 2012). In line with these differential mechanisms of soluble vs. insoluble Aβ species, the effect of Aβ peptides on mitochondrial dynamics and function was also reported to depend on the peptide structure (Calkins and Reddy, 2011; Decker et al., 2010; Meyer-Luehmann et al., 2008; Pigino et al., 2009; Poon et al., 2011; Poon et al., 2013; Ramser et al., 2013; Rui et al., 2010; Rui et al., 2006; Rui and Zheng, 2016; Trushina et al., 2012; Wang et al., 2010). The strength of our study is in comparing side by side the effect of multiple Aβ peptides on mitochondrial motility in live neurons using a standardized assay; in a comprehensive characterization of the peptide structure in dynamic relationship to the effect on axonal trafficking and function using variety of biochemical techniques; and in the utilization of multiple peptides including Aβ40, Aβ42, Aβ39E22, Aβ40H13G, Aβ40A2T in soluble and fibrillar forms. Our data suggest that all soluble peptides excluding Aβ40H13G caused inhibition of axonal trafficking of mitochondria. However, the impact on mitochondrial motility directly correlated with the propensity of these peptides to aggregate. The comparison of structural data obtained with dynamic light scattering, AFM, and TEM demonstrated significantly higher tendency of Aβ42 and Aβ39E22 to form high molecular weight species immediately after the preparation compared to Aβ40, which formed a mixture of monomers and oligomers. Similar results were obtained for all fibrillar Aβ peptides tested in our study. Irrelevant of the peptide origin, fibrillar peptides impacted axonal trafficking to the significantly greater extent than their soluble forms. This observation is supported by recent reports demonstrating that Aβ fibrils and not oligomers foist a specific effect on cellular plasma membrane affecting the composition of lipid rafts. Interestingly, this interaction with the plasma membrane occurred without penetrating the cells or permeabilizing them to Ca^{2+} entry (Bucciantini et al., 2012; Okada et al., 2008).

Mitochondria are sensitive to the calcium levels in the cell, and their transportation to and localization at the sites of calcium entry is essential for proper calcium buffering (Wang and Schwarz, 2009). Mitochondrial transport machinery includes bidirectional trafficking in anterograde and retrograde directions. The pattern of mitochondrial motility is rather chaotic: they could move in each direction in a steady, smooth fashion; display a stop-and-go motion with frequent changes in directions; and at any given time, the majority of organelles is stationary displaying a very subtle, salutatory movement without a net direction (Trushina et al., 2004; Trushina et al., 2012). Molecular complexes that include kinesin superfamily proteins or dynein protein facilitate transport of mitochondria in anterograde and retrograde directions, respectively. All of these motor proteins hydrolase ATP to complete the task (Martin et al., 1999). Regulation of mitochondrial transport is complex, appears to be specific for a particular neuronal compartment (dendrites vs. axons), and is not well understood. Emerging findings demonstrate that mitochondrial distribution in neurons is correlated with synaptic activity where organelle's motility is directed by ATP, ADP and calcium levels (MacAskill and Kittler, 2010). In addition, mitochondrial trafficking and docking could be regulated by the nerve growth factor (NGF), phosphoinositide 3-kinase (PI3K) and AKT–glycogen synthase kinase 3β (GSK3β) signaling (Chada and Hollenbeck, 2003; Chada and Hollenbeck, 2004; Chen et al., 2007). Furthermore, since mitochondria primarily move along microtubules, it is not surprising that microtubule-associated proteins

were also found to be involved in the regulation of mitochondrial trafficking. Thus, trafficking of mitochondria was particular sensitive to the levels of Tau protein where its overexpression specifically inhibited mitochondria movement in anterograde direction (Dubey et al., 2008; Stamer et al., 2002; Stoothoff et al., 2009). In our experiments, where the effect of acute treatment with exogenous Aβ peptides on mitochondrial motility was tested within 30 min after the peptide addition, we did not detect any changes in the levels of pTau, PI3K or GSK3β (data not shown). However, there is a strong evidence that the molecular mechanisms of trafficking inhibition depend on the state of Aβ aggregation. We and others have observed that inhibition of mitochondrial motility occurs within minutes after the addition of exogenous Aβ peptides suggesting the initiating of a signaling cascade at the plasma membrane (Rui et al., 2006). However, experiments in isolated squid axoplasm where a perfusion with Aβ peptides caused a bidirectional inhibition of axonal transport suggest the existence of an additional plasma membrane–independent mechanism (Pigino et al., 2009). Thus, it is feasible that exogenous and endogenous Aβ peptides facilitate mitochondrial trafficking inhibition via different mechanisms. In support, our examination of the effect of Aβ40H13G peptide with reduced plasma membrane binding on mitochondrial motility in neurons revealed a total lack of trafficking inhibition regardless of the peptide concentration. Moreover, capture of Aβ42 peptides with specific antibody IgG4.1 (Poduslo et al., 2007; Ramakrishnan et al., 2009) also blocked the effect on axonal trafficking suggesting that binding to the plasma membrane is essential to cause trafficking deficit in neurons. We have previously demonstrated that early stage and late stage fibrils of Aβ39E22 have enhanced neuronal binding with subsequent accumulation in lysosomes (Poduslo et al., 2012). The present study confirms that the enhanced aggregation capacity and plasma membrane binding of fibrillar Aβ39E22 must exert a stronger inhibitory effect on mitochondrial trafficking compared to Aβ40 peptides. Taking together, these data imply that Aβ may impact trafficking machinery in multiple ways. The extracellular Aβ could initiate a signaling cascade by binding to the plasma membrane, while after internalization it may also exacerbate trafficking inhibition by directly impacting motor proteins and/or mitochondria in the cytoplasm (Hansson Petersen et al., 2008a; Pigino et al., 2009; Pigino et al., 2003). The stronger inhibitory effect of Aβ fibrils is consistent with the hypothesis that inhibition of axonal transport requires activation of a signaling cascade through particular receptors at the plasma membrane. Indeed, activation of pathways that involve GSK3β, JNK and Cdk5 kinases were proposed to play a role in axonal trafficking inhibition in AD (Morfini et al., 2002; Muresan and Muresan, 2012; Pigino et al., 2003; Rui et al., 2010; Rui et al., 2006). In this case, fibrils could cause an amplified response by affecting larger number of plasma membrane receptors compared to Aβ monomers or oligomers. Moreover, we have previously demonstrated that different Aβ peptides are internalized in neurons via different endocytic mechanisms. Interaction of Aβ peptides with distinctive areas of the plasma membrane such as lipid rafts that are involved in facilitating the specific signaling cascades could also account for different and peptide-specific mechanisms of axonal trafficking inhibition. Furthermore, Aβ binding to cellular prion protein (PrP[C]) (Walsh et al., 2014) or β1-integrin acivates cofilin (Woo et al., 2015) leading to a formation of bundles of filaments (rods) containing cofilin:actin (1:1), which disrupts dendritic microtubule integrity and blocks intracellular trafficking of mitochondria and early endosomes (Cichon et al., 2012; Davis et al., 2011). Finally, our data demonstrate that Icelandic Aβ peptide with

protective A673T mutation affects axonal trafficking of mitochondria and increases the number of stationary organelles similar to other Aβ peptides. This variant is associated with minimal amyloid deposition and significantly reduced amyloid production (Benilova et al., 2014; Maloney et al., 2014; Zheng et al., 2015). Therefore, these properties together with its significantly reduced binding to neuronal plasma membrane could account for the lack of pronounced pathological effect on mitochondrial trafficking since this peptide could be cleared from the brain prior to imparting mitochondrial dysfunction.

Accumulation of extracellular secreted pathogenic Aβ in neurons was reported early in AD progression prior to the onset of AD phenotype (Echeverria and Cuello, 2002; Gouras et al., 2005; Kandimalla et al., 2009). Our data is consistent with the mechanism where soluble Aβ monomers and oligomers formed early in AD inhibit mitochondrial trafficking by binding to the plasma membrane and internalizing via energy dependent and/or independent mechanisms (Jungbauer et al., 2009; Kandimalla et al., 2009). Later in the disease, formation of extracellular plaques and Aβ fibrils could additionally exacerbate trafficking phenotype in neurons, especially affecting neuropils in close proximity to plaques. Indeed, we directly observed the interaction of Aβ fibrils with mitochondria - containing neuropils in the brain tissue of the APP/PS1 mice using TEM. Taken together, our data suggest that early in AD development, axonal transport could be primarily affected by soluble Aβ monomers and oligomers while during the disease progression the formation of extracellular aggregates and fibrils could exacerbate trafficking phenotype. This is in agreement with the data demonstrating that axonal trafficking is already affected in embryonic neurons in mouse models of AD where, at that stage of the disease progression, formation of aggregated Aβ is not observed (Trushina et al., 2012). Later in the disease, aggregated Aβ peptides could exacerbate axonal transport deficiency in neurons located in proximity to the amyloid plaques contributing to the accelerated neuronal loss. Since we have found that Aβ monomers along with oligomers significantly impact axonal trafficking, strategies designed to block Aβ oligomerization or fibrillization alone without ensuring the efficient clearance of Aβ monomers may not be sufficient to alleviate trafficking phenotype. However, our data demonstrate that trafficking inhibition does not cause the loss of mitochondrial function providing a compelling evidence for spatial separation of these two events in disease progression and validating restoration of axonal trafficking as a therapeutic strategy for AD. However, the scope of our study was on the evaluation of the ability of mitochondria to produce energy and maintain bioenergetic parameters that could be measured using a Seahorse Extracellular Flux Analyzer. It remains to be determined to what extent and at what time the exposure to various peptides affects mitochondrial ROS production or calcium buffering in respect to changes in axonal trafficking. Our data are consistent with recently reported observations that anterograde and retrograde transport of brain-derived neurotrophic factor (BDNF) - containing vesicles but not the activity-dependent release of BDNF from these vesicles was affected after the acute treatment with Aβ42 peptides in neurons (Seifert et al., 2016). Indeed, we have shown that partial inhibition of mitochondrial complex I with small molecules induces a positive metabolic adaptation resulting in a reduction of pTau and Aβ levels, and the activity of GSK3β in multiple mouse models of AD (Zhang et al., 2015). When breeding APP and PS1 mice were treated with this compound, axonal trafficking of mitochondria was completely restored in primary neurons

from progeny while in untreated mice it was severely affected (Trushina et al., 2012; Zhang et al., 2015). Moreover, AD mice born from the drug-treated parents had significantly delayed onset of cognitive and behavior phenotype (Zhang et al., 2015). Analysis of the brain tissue from these mice revealed increased levels of BDNF and synaptic proteins, and enhanced cellular energetics associated with cognitive protection. Similar, restoration of axonal trafficking using antioxidants, by increasing the acetylation of anti-oxidant protein peroxdiredoxin1 by HDAC6 inhibition or by treatment with genipiside, a pharmacologically active component purified from gardenia fruit, resulted in reduced levels of ROS and Ca^{2+}, and synaptic protection in multiple cellular and mouse models of AD (Choi et al., 2017; Guo et al., 2013; Lv et al., 2015; Reddy et al., 2012; Yu et al., 2016; Zhang et al., 2016a). Since mitochondrial trafficking inhibition in neurons is not specific to AD (De Vos and Hafezparast, 2017; Morfini et al., 2009; Trushina et al., 2004), the development of therapeutic strategies to restore axonal trafficking could be beneficial for multiple neurodegenerative diseases.

5. Conclusions

Aβ peptides including Icelandic peptide inhibit axonal trafficking of mitochondria regardless of their aggregated state and solubility. Peptides with high propensity to aggregate and fibrils affect axonal trafficking to the greater extent. Binding to the plasma membrane is sufficient to cause trafficking inhibition. There is a spatial separation between Aβ-induced inhibition of axonal transport and the loss of mitochondrial bioenergetics. Therapeutic approaches focused on the restoration of axonal trafficking may be specifically efficient at the early stages of multiple neurodegenerative diseases where mitochondrial function is mainly preserved.

Acknowledgments

Abbreviations

Aβ	amyloid beta
AD	Alzheimer's Disease
AFM	atomic force microscopy
AFU	arbitrary fluorescence units
AKT	Protein kinase B

APP	amyloid precursor protein
Aβ	amyloid beta
BACE1	β-APP cleaving enzyme
BDNF	brain-derived neurotrophic factor
EM	electron microscopy
ER	Endoplasmic Reticulum
ETC	electron transport chain
FAD	familial Alzheimer's Disease
F-Aβ40	fluorescently labeled Aβ40
F-Aβ40A2T	fluorescently labeled Aβ40A2T
FCCP	carbonyl cyanide-*p*-trifluoromethoxyphenylhydrazone
GSK3β	glycogen synthase kinase 3β
HD	Huntington's Disease
JNK	Jun N-terminal kinases
LSM	Laser scanning microscope
MM SPM	MultiMode Scanning Probe Microscope
MRC	maximal respiratory capacity
MVB	multivesicular bodies
NFT	neurofibrillary tangles
NGF	nerve growth factor
OCR	Oxygen Consumption Rate
OXPHOS	oxidative phosphorylation
PD	Parkinson's Diseases
PI3K	phosphoinositide 3-kinase
PS1 and 2	presenilin 1 and 2
ROS	reactive oxygen species
Seahorse XF24	a Seahorse Extracellular Flux Analyzer
SRC	spare respiratory capacity
TEM	transmission electron microscopy

TGN	trans-Golgi network
TMRM	tetramethylrhodamine, methyl ester

References

Alzheimer's Association. Alzheimer's Disease Facts and Figures. 2017. alz.org/facts

Area-Gomez E, Schon EA. 2017; On the pathogenesis of Alzheimer's disease: the MAM hypothesis. FASEB J. 31 :864–867. [PubMed: 28246299]

Beal MF. 2005; Mitochondria take center stage in aging and neurodegeneration. Ann Neurol. 58 :495–505. [PubMed: 16178023]

Benilova I, et al. 2012; The toxic Abeta oligomer and Alzheimer's disease: an emperor in need of clothes. Nat Neurosci. 15 :349–357. [PubMed: 22286176]

Benilova I, et al. 2014; The Alzheimer disease protective mutation A2T modulates kinetic and thermodynamic properties of amyloid-beta (Abeta) aggregation. J Biol Chem. 289 :30977–30989. [PubMed: 25253695]

Benseny-Cases N, et al. 2012; In vitro oligomerization and fibrillogenesis of amyloid-beta peptides. Subcell Biochem. 65 :53–74. [PubMed: 23224999]

Bossy-Wetzel E, et al. 2004; Molecular pathways to neurodegeneration. Nat Med. 10 (Suppl) :S2–9. [PubMed: 15272266]

Brand MD, Nicholls DG. 2011; Assessing mitochondrial dysfunction in cells. Biochem J. 435 :297–312. [PubMed: 21726199]

Bucciantini M, et al. 2012; Toxic effects of amyloid fibrils on cell membranes: the importance of ganglioside GM1. FASEB J. 26 :818–831. [PubMed: 22071505]

Busciglio J, et al. 1993; Generation of beta-amyloid in the secretory pathway in neuronal and nonneuronal cells. Proc Natl Acad Sci U S A. 90 :2092–2096. [PubMed: 8446635]

Calkins MJ, Reddy PH. 2011; Amyloid beta impairs mitochondrial anterograde transport and degenerates synapses in Alzheimer's disease neurons. Biochim Biophys Acta. 1812 :507–513. [PubMed: 21241801]

Calkins MJ, et al. 2011; Impaired mitochondrial biogenesis, defective axonal transport of mitochondria, abnormal mitochondrial dynamics and synaptic degeneration in a mouse model of Alzheimer's disease. Hum Mol Genet. 20 :4515–4529. [PubMed: 21873260]

Canevari L, et al. 2004; Toxicity of amyloid beta peptide: tales of calcium, mitochondria, and oxidative stress. Neurochem Res. 29 :637–650. [PubMed: 15038611]

Caspersen C, et al. 2005; Mitochondrial Abeta: a potential focal point for neuronal metabolic dysfunction in Alzheimer's disease. FASEB J. 19 :2040–2041. [PubMed: 16210396]

Cha MY, et al. 2012; Mitochondria-specific accumulation of amyloid beta induces mitochondrial dysfunction leading to apoptotic cell death. PLoS One. 7 :e34929. [PubMed: 22514691]

Chada SR, Hollenbeck PJ. 2003; Mitochondrial movement and positioning in axons: the role of growth factor signaling. J Exp Biol. 206 :1985–1992. [PubMed: 12756280]

Chada SR, Hollenbeck PJ. 2004; Nerve growth factor signaling regulates motility and docking of axonal mitochondria. Curr Biol. 14 :1272–1276. [PubMed: 15268858]

Chen H, Chan DC. 2009; Mitochondrial dynamics–fusion, fission, movement, and mitophagy–in neurodegenerative diseases. Hum Mol Genet. 18 :R169–76. [PubMed: 19808793]

Chen JX, Yan SS. 2010; Role of mitochondrial amyloid-beta in Alzheimer's disease. J Alzheimers Dis. 20 (Suppl 2) :S569–78. [PubMed: 20463403]

Chen S, et al. 2007; Serotonin stimulates mitochondrial transport in hippocampal neurons. Mol Cell Neurosci. 36 :472–483. [PubMed: 17904380]

Choi SW, et al. 2009; Bioenergetic analysis of isolated cerebrocortical nerve terminals on a microgram scale: spare respiratory capacity and stochastic mitochondrial failure. J Neurochem. 109 :1179–1191. [PubMed: 19519782]

Choi H, et al. 2017; Increased acetylation of Peroxiredoxin1 by HDAC6 inhibition leads to recovery of Abeta-induced impaired axonal transport. Mol Neurodegener. 12 :23. [PubMed: 28241840]

Cichon J, et al. 2012; Cofilin aggregation blocks intracellular trafficking and induces synaptic loss in hippocampal neurons. J Biol Chem. 287 :3919–3929. [PubMed: 22184127]

Cloe AL, et al. 2011; The Japanese mutant Abeta (DeltaE22-Abeta(1-39)) forms fibrils instantaneously, with low-thioflavin T fluorescence: seeding of wild-type Abeta(1-40) into atypical fibrils by DeltaE22-Abeta(1-39). Biochemistry. 50 :2026–2039. [PubMed: 21291268]

Cohen SI, et al. 2013; Proliferation of amyloid-beta42 aggregates occurs through a secondary nucleation mechanism. Proc Natl Acad Sci U S A. 110 :9758–9763. [PubMed: 23703910]

Correia SC, et al. 2016; Mitochondrial traffic jams in Alzheimer's disease - pinpointing the roadblocks. Biochim Biophys Acta. 1862 :1909–1917. [PubMed: 27460705]

Davis RC, et al. 2011; Amyloid beta dimers/trimers potently induce cofilin-actin rods that are inhibited by maintaining cofilin-phosphorylation. Mol Neurodegener. 6 :10. [PubMed: 21261978]

De Vos KJ, Hafezparast M. 2017; Neurobiology of axonal transport defects in motor neuron diseases: opportunities for translational research? Neurobiol. Dis. 105 :283–299.

Decker H, et al. 2010; Amyloid-beta peptide oligomers disrupt axonal transport through an NMDA receptor-dependent mechanism that is mediated by glycogen synthase kinase 3beta in primary cultured hippocampal neurons. J Neurosci. 30 :9166–9171. [PubMed: 20610750]

Dubey M, et al. 2008; Tau inhibits anterograde axonal transport and perturbs stability in growing axonal neurites in part by displacing kinesin cargo: neurofilaments attenuate tau-mediated neurite instability. Cell Motil Cytoskeleton. 65 :89–99. [PubMed: 18000878]

Duff K, et al. 1996; Increased amyloid-beta42(43) in brains of mice expressing mutant presenilin 1. Nature. 383 :710–713. [PubMed: 8878479]

Echeverria V, Cuello AC. 2002; Intracellular A-beta amyloid, a sign for worse things to come? Mol. Neurobiol. 26 :299–316.

Ehehalt R, et al. 2003; Amyloidogenic processing of the Alzheimer beta-amyloid precursor protein depends on lipid rafts. J Cell Biol. 160 :113–123. [PubMed: 12515826]

El-Kadi AM, et al. 2007; Defective axonal transport in motor neuron disease. J Neurosci Res. 85 :2557–2566. [PubMed: 17265455]

Galindo MF, et al. 2010; Mitochondrial biology in Alzheimer's disease pathogenesis. J Neurochem. 114 :933–945. [PubMed: 20492350]

Gerencser AA, et al. 2009; Quantitative microplate-based respirometry with correction for oxygen diffusion. Anal Chem. 81 :6868–6878. [PubMed: 19555051]

Goldstein LS. 2012; Axonal transport and neurodegenerative disease: can we see the elephant? Prog. Neurobiol. 99 :186–190.

Gouras GK, et al. 2005; Intraneuronal Abeta accumulation and origin of plaques in Alzheimer's disease. Neurobiol Aging. 26 :1235–1244. [PubMed: 16023263]

Greenfield JP, et al. 1999; Endoplasmic reticulum and trans-Golgi network generate distinct populations of Alzheimer beta-amyloid peptides. Proc Natl Acad Sci U S A. 96 :742–747. [PubMed: 9892704]

Guo L, et al. 2013; Cyclophilin D deficiency rescues axonal mitochondrial transport in Alzheimer's neurons. PLoS One. 8 :e54914. [PubMed: 23382999]

Hansson Petersen CA, et al. 2008a; The amyloid beta-peptide is imported into mitochondria via the TOM import machinery and localized to mitochondrial cristae. Proc Natl Acad Sci U S A. 105 :13145–13150. [PubMed: 18757748]

Hansson Petersen CA, et al. 2008b; The amyloid beta-peptide is imported into mitochondria via the TOM import machinery and localized to mitochondrial cristae. Proc Natl Acad Sci U S A. 105 :13145–13150. [PubMed: 18757748]

Hatami A, et al. 2017; Familial Alzheimer's disease mutations within the amyloid precursor protein Alter the aggregation and conformation of the amyloid-beta peptide. J Biol Chem. 292 :3172–3185. [PubMed: 28049728]

Hellstrand E, et al. 2010; Amyloid beta-protein aggregation produces highly reproducible kinetic data and occurs by a two-phase process. ACS Chem Neurosci. 1 :13–18. [PubMed: 22778803]

Holcomb L, et al. 1998; Accelerated Alzheimer-type phenotype in transgenic mice carrying both mutant amyloid precursor protein and presenilin 1 transgenes. Nat Med. 4 :97–100. [PubMed: 9427614]

Hollenbeck PJ. 1996; The pattern and mechanism of mitochondrial transport in axons. Front Biosci. 1 :d91–102. [PubMed: 9159217]

Hollenbeck PJ, Saxton WM. 2005; The axonal transport of mitochondria. J Cell Sci. 118 :5411–5419. [PubMed: 16306220]

Hsiao K, et al. 1996; Correlative memory deficits, Abeta elevation, and amyloid plaques in transgenic mice. Science. 274 :99–102. [PubMed: 8810256]

Iijima-Ando K, et al. 2009; Mitochondrial mislocalization underlies Abeta42-induced neuronal dysfunction in a drosophila model of Alzheimer's disease. PLoS One. 4 :e8310. [PubMed: 20016833]

Itoh K, et al. 2013; Mitochondrial dynamics in neurodegeneration. Trends Cell Biol. 23 :64–71. [PubMed: 23159640]

Ittner LM, et al. 2010; Dendritic function of tau mediates amyloid-beta toxicity in Alzheimer's disease mouse models. Cell. 142 :387–397. [PubMed: 20655099]

Jack CR Jr, et al. 2014; Rates of beta-amyloid accumulation are independent of hippocampal neurodegeneration. Neurology. 82 :1605–1612. [PubMed: 24706010]

Jin M, et al. 2011; Soluble amyloid beta-protein dimers isolated from Alzheimer cortex directly induce tau hyperphosphorylation and neuritic degeneration. Proc Natl Acad Sci U S A. 108 :5819–5824. [PubMed: 21421841]

Jonsson T, et al. 2012; A mutation in APP protects against Alzheimer's disease and age-related cognitive decline. Nature. 488 :96–99. [PubMed: 22801501]

Jungbauer LM, et al. 2009; Preparation of fluorescently-labeled amyloid-beta peptide assemblies: the effect of fluorophore conjugation on structure and function. J Mol Recognit. 22 :403–413. [PubMed: 19343729]

Kandimalla KK, et al. 2009; Mechanism of neuronal versus endothelial cell uptake of Alzheimer's disease amyloid beta protein. PLoS One. 4 :e4627. [PubMed: 19247480]

Karran E, et al. 2011; The amyloid cascade hypothesis for Alzheimer's disease: an appraisal for the development of therapeutics. Nat Rev Drug Discov. 10 :698–712. [PubMed: 21852788]

Kassler K, et al. 2010; Effect of pathogenic mutations on the structure and dynamics of Alzheimer's A beta 42-amyloid oligomers. J Mol Model. 16 :1011–1020. [PubMed: 19908073]

Kepp KP. 2017; Ten challenges of the amyloid hypothesis of Alzheimer's disease. J Alzheimers Dis. 55 :447–457. [PubMed: 27662304]

Kokawa A, et al. 2015; The A673T mutation in the amyloid precursor protein reduces the production of beta-amyloid protein from its beta-carboxyl terminal fragment in cells. Acta Neuropathol Commun. 3 :66. [PubMed: 26531305]

Lacor PN, et al. 2004; Synaptic targeting by Alzheimer's-related amyloid beta oligomers. J Neurosci. 24 :10191–10200. [PubMed: 15537891]

LaFerla FM, et al. 2007; Intracellular amyloid-beta in Alzheimer's disease. Nat Rev Neurosci. 8 :499–509. [PubMed: 17551515]

Lange M, et al. 2012; Comprehensive method for culturing embryonic dorsal root ganglion neurons for seahorse extracellular flux XF24 analysis. Front Neurol. 3 :175. [PubMed: 23248613]

Lin MY, et al. 2017; Releasing syntaphilin removes stressed mitochondria from axons independent of mitophagy under pathophysiological conditions. Neuron. 94 (595–610) :e6.

Lv C, et al. 2015; Multi-faced neuroprotective effects of geniposide depending on the RAGE-mediated signaling in an Alzheimer mouse model. Neuropharmacology. 89 :175–184. [PubMed: 25261783]

MacAskill AF, Kittler JT. 2010; Control of mitochondrial transport and localization in neurons. Trends Cell Biol. 20 :102–112. [PubMed: 20006503]

Mairet-Coello G, et al. 2013; The CAMKK2-AMPK kinase pathway mediates the synaptotoxic effects of Abeta oligomers through Tau phosphorylation. Neuron. 78 :94–108. [PubMed: 23583109]

Maloney JA, et al. 2014; Molecular mechanisms of Alzheimer disease protection by the A673T allele of amyloid precursor protein. J Biol Chem. 289 :30990–31000. [PubMed: 25253696]

Mar FM, et al. 2014; CNS axons globally increase axonal transport after peripheral conditioning. J Neurosci. 34 :5965–5970. [PubMed: 24760855]

Martin M, et al. 1999; Cytoplasmic dynein, the dynactin complex, and kinesin are interdependent and essential for fast axonal transport. Mol Biol Cell. 10 :3717–3728. [PubMed: 10564267]

Masuda Y, et al. 2008; Verification of the intermolecular parallel beta-sheet in E22K-Abeta42 aggregates by solid-state NMR using rotational resonance: implications for the supramolecular arrangement of the toxic conformer of Abeta42. Biosci Biotechnol Biochem. 72 :2170–2175. [PubMed: 18685204]

Meyer-Luehmann M, et al. 2008; Rapid appearance and local toxicity of amyloid-beta plaques in a mouse model of Alzheimer's disease. Nature. 451 :720–724. [PubMed: 18256671]

Millecamps S, Julien JP. 2013; Axonal transport deficits and neurodegenerative diseases. Nat Rev Neurosci. 14 :161–176. [PubMed: 23361386]

Miller EC, et al. 2014; Tau phosphorylation and tau mislocalization mediate soluble Abeta oligomer-induced AMPA glutamate receptor signaling deficits. Eur J Neurosci. 39 :1214–1224. [PubMed: 24713000]

Morfini G, et al. 2002; Fast axonal transport misregulation and Alzheimer's disease. NeuroMolecular Med. 2 :89–99. [PubMed: 12428805]

Morfini GA, et al. 2009; Axonal transport defects in neurodegenerative diseases. J Neurosci. 29 :12776–12786. [PubMed: 19828789]

Mossmann D, et al. 2014; Amyloid-beta peptide induces mitochondrial dysfunction by inhibition of preprotein maturation. Cell Metab. 20 :662–669. [PubMed: 25176146]

Muresan V, Muresan Z. 2012; A persistent stress response to impeded axonal transport leads to accumulation of amyloid-beta in the endoplasmic reticulum, and is a probable cause of sporadic Alzheimer's disease. Neurodegener Dis. 10 :60–63. [PubMed: 22156573]

Nicholls DG, et al. 2010; Bioenergetic profile experiment using C2C12 myoblast cells. J Vis Exp. 46 :2511–2516.

Nilsberth C, et al. 2001; The 'Arctic' APP mutation (E693G) causes Alzheimer's disease by enhanced Abeta protofibril formation. Nat Neurosci. 4 :887–893. [PubMed: 11528419]

Nishitsuji K, et al. 2009; The E693Delta mutation in amyloid precursor protein increases intracellular accumulation of amyloid beta oligomers and causes endoplasmic reticulum stress-induced apoptosis in cultured cells. Am J Pathol. 174 :957–969. [PubMed: 19164507]

O'Brien RJ, Wong PC. 2011; Amyloid precursor protein processing and Alzheimer's disease. Annu Rev Neurosci. 34 :185–204. [PubMed: 21456963]

Okada T, et al. 2008; Formation of toxic Abeta(1-40) fibrils on GM1 ganglioside-containing membranes mimicking lipid rafts: polymorphisms in Abeta(1-40) fibrils. J Mol Biol. 382 :1066–1074. [PubMed: 18692507]

Ovchinnikova OY, et al. 2011; The Osaka FAD mutation E22Delta leads to the formation of a previously unknown type of amyloid beta fibrils and modulates Abeta neurotoxicity. J Mol Biol. 408 :780–791. [PubMed: 21402079]

Overly CC, et al. 1996; Organelle motility and metabolism in axons vs dendrites of cultured hippocampal neurons. J Cell Sci. 109 (Pt 5) :971–980. [PubMed: 8743944]

Palau F, et al. 2009; The role of mitochondrial network dynamics in the pathogenesis of Charcot-Marie-tooth disease. Adv Exp Med Biol. 652 :129–137. [PubMed: 20225023]

Pigino G, et al. 2003; Alzheimer's presenilin 1 mutations impair kinesin-based axonal transport. J Neurosci. 23 :4499–4508. [PubMed: 12805290]

Pigino G, et al. 2009; Disruption of fast axonal transport is a pathogenic mechanism for intraneuronal amyloid beta. Proc Natl Acad Sci U S A. 106 :5907–5912. [PubMed: 19321417]

Pimplikar SW, et al. 2010; Amyloid-independent mechanisms in Alzheimer's disease pathogenesis. J Neurosci. 30 :14946–14954. [PubMed: 21068297]

Poduslo JF, et al. 2007; In vivo targeting of antibody fragments to the nervous system for Alzheimer's disease immunotherapy and molecular imaging of amyloid plaques. J Neurochem. 102 :420–433. [PubMed: 17596213]

Poduslo JF, et al. 2010; HH domain of Alzheimer's disease Abeta provides structural basis for neuronal binding in PC12 and mouse cortical/hippocampal neurons. PLoS One. 5 :e8813. [PubMed: 20098681]

Poduslo JF, et al. 2012; Alzheimer's disease amyloid beta-protein mutations and deletions that define neuronal binding/internalization as early stage nonfibrillar/fibrillar aggregates and late stage fibrils. Biochemistry. 51 :3993–4003. [PubMed: 22545812]

Poon WW, et al. 2011; beta-Amyloid impairs axonal BDNF retrograde trafficking. Neurobiol Aging. 32 :821–833. [PubMed: 19540623]

Poon WW, et al. 2013; beta-Amyloid (Abeta) oligomers impair brain-derived neurotrophic factor retrograde trafficking by down-regulating ubiquitin C-terminal hydrolase, UCH-L1. J Biol Chem. 288 :16937–16948. [PubMed: 23599427]

Querfurth HW, LaFerla FM. 2010; Alzheimer's disease. N Engl J Med. 362 :329–344. [PubMed: 20107219]

Rajendran L, et al. 2006; Alzheimer's disease beta-amyloid peptides are released in association with exosomes. Proc Natl Acad Sci U S A. 103 :11172–11177. [PubMed: 16837572]

Ramakrishnan M, et al. 2008; Selective contrast enhancement of individual Alzheimer's disease amyloid plaques using a polyamine and Gd-DOTA conjugated antibody fragment against fibrillar Abeta42 for magnetic resonance molecular imaging. Pharm Res. 25 :1861–1872. [PubMed: 18443900]

Ramakrishnan M, et al. 2009; Surface plasmon resonance binding kinetics of Alzheimer's disease amyloid beta peptide-capturing and plaque-binding monoclonal antibodies. Biochemistry. 48 :10405–10415. [PubMed: 19775170]

Ramser EM, et al. 2013; Amyloid-beta oligomers induce tau-independent disruption of BDNF axonal transport via calcineurin activation in cultured hippocampal neurons. Mol Biol Cell. 24 :2494–2505. [PubMed: 23783030]

Reddy PH, et al. 2010; Amyloid-beta and mitochondria in aging and Alzheimer's disease: implications for synaptic damage and cognitive decline. J Alzheimers Dis. 20 (Suppl 2) :S499–512. [PubMed: 20413847]

Reddy PH, et al. 2012; Abnormal mitochondrial dynamics and synaptic degeneration as early events in Alzheimer's disease: implications to mitochondria-targeted anti-oxidant therapeutics. Biochim Biophys Acta. 1822 :639–649. [PubMed: 22037588]

Rui Y, Zheng JQ. 2016; Amyloid beta oligomers elicit mitochondrial transport defects and fragmentation in a time-dependent and pathway-specific manner. Mol Brain. 9 :79. [PubMed: 27535553]

Rui Y, et al. 2006; Acute impairment of mitochondrial trafficking by beta-amyloid peptides in hippocampal neurons. J Neurosci. 26 :10480–10487. [PubMed: 17035532]

Rui Y, et al. 2010; Inhibition of AMPA receptor trafficking at hippocampal synapses by beta-amyloid oligomers: the mitochondrial contribution. Mol Brain. 3 :10. [PubMed: 20346152]

Sansbury BE, et al. 2011; Bioenergetic function in cardiovascular cells: the importance of the reserve capacity and its biological regulation. Chem Biol Interact. 191 :288–295. [PubMed: 21147079]

Schwarz TL. 2013 Mitochondrial trafficking in neurons. Cold Spring Harb Perspect Biol. :5.

Seifert B, et al. 2016; Amyloid-beta induced changes in vesicular transport of BDNF in hippocampal neurons. Neural Plast. 2016 :4145708. [PubMed: 26881108]

Selfridge JE, et al. 2013; Role of mitochondrial homeostasis and dynamics in Alzheimer's disease. Neurobiol Dis. 51 :3–12. [PubMed: 22266017]

Selkoe DJ. 2003; Folding proteins in fatal ways. Nature. 426 :900–904. [PubMed: 14685251]

Shankar GM, et al. 2008; Amyloid-beta protein dimers isolated directly from Alzheimer's brains impair synaptic plasticity and memory. Nat Med. 14 :837–842. [PubMed: 18568035]

Sheng ZH, Cai Q. 2012; Mitochondrial transport in neurons: impact on synaptic homeostasis and neurodegeneration. Nat Rev Neurosci. 13 :77–93. [PubMed: 22218207]

Stamer K, et al. 2002; Tau blocks traffic of organelles, neurofilaments, and APP vesicles in neurons and enhances oxidative stress. J Cell Biol. 156 :1051–1063. [PubMed: 11901170]

Stoothoff W, et al. 2009; Differential effect of three-repeat and four-repeat tau on mitochondrial axonal transport. J Neurochem. 111 :417–427. [PubMed: 19686388]

Swerdlow RH, et al. 2014; The Alzheimer's disease mitochondrial cascade hypothesis: progress and perspectives. Biochim Biophys Acta. 1842 :1219–1231. [PubMed: 24071439]

Swomley AM, et al. 2014; Abeta, oxidative stress in Alzheimer disease: evidence based on proteomics studies. Biochim Biophys Acta. 1842 :1248–1257. [PubMed: 24120836]

Tillement L, et al. 2011; Alzheimer's disease: effects of beta-amyloid on mitochondria. Mitochondrion. 11 :13–21. [PubMed: 20817045]

Tomiyama T, et al. 2008; A new amyloid beta variant favoring oligomerization in Alzheimer's-type dementia. Ann Neurol. 63 :377–387. [PubMed: 18300294]

Tonnies E, Trushina E. 2017; Oxidative stress, synaptic dysfunction, and Alzheimer's disease. J Alzheimers Dis. 57 :1105–1121. [PubMed: 28059794]

Trushina E, et al. 2003; Microtubule destabilization and nuclear entry are sequential steps leading to toxicity in Huntington's disease. Proc Natl Acad Sci U S A. 100 :12171–12176. [PubMed: 14527999]

Trushina E, et al. 2004; Mutant huntingtin impairs axonal trafficking in mammalian neurons in vivo and in vitro. Mol Cell Biol. 24 :8195–8209. [PubMed: 15340079]

Trushina E, et al. 2006; Mutant huntingtin inhibits clathrin-independent endocytosis and causes accumulation of cholesterol in vitro and in vivo. Hum Mol Genet. 15 :3578–3591. [PubMed: 17142251]

Trushina E, et al. 2012 Defects in mitochondrial dynamics and metabolomic signatures of evolving energetic stress in mouse models of familial Alzheimer's disease. PLoS One. :7.

Tsigelny IF, et al. 2014; Structural diversity of Alzheimer's disease amyloid-beta dimers and their role in oligomerization and fibril formation. J Alzheimers Dis. 39 :583–600. [PubMed: 24240640]

Verma M, et al. 2015; Toxic species in amyloid disorders: oligomers or mature fibrils. Ann Indian Acad Neurol. 18 :138–145. [PubMed: 26019408]

Verpillot R, et al. 2008; Simultaneous analysis by capillary electrophoresis of five amyloid peptides as potential biomarkers of Alzheimer's disease. J Chromatogr A. 1214 :157–164. [PubMed: 18992892]

Walsh KP, et al. 2014; Amyloid-beta and proinflammatory cytokines utilize a prion protein-dependent pathway to activate NADPH oxidase and induce cofilin-actin rods in hippocampal neurons. PLoS One. 9 :e95995. [PubMed: 24760020]

Wang X, Schwarz TL. 2009; The mechanism of Ca2+ - dependent regulation of kinesin-mediated mitochondrial motility. Cell. 136 :163–174. [PubMed: 19135897]

Wang X, et al. 2010; Amyloid-beta-derived diffusible ligands cause impaired axonal transport of mitochondria in neurons. Neurodegener Dis. 7 :56–59. [PubMed: 20160460]

Wirths O, et al. 2004; A modified beta-amyloid hypothesis: intraneuronal accumulation of the beta-amyloid peptide–the first step of a fatal cascade. J Neurochem. 91 :513–520. [PubMed: 15485483]

Woo JA, et al. 2015; Slingshot-Cofilin activation mediates mitochondrial and synaptic dysfunction via Abeta ligation to beta1-integrin conformers. Cell Death Differ. 22 :1069–1070. [PubMed: 25941167]

Yao J, Brinton RD. 2011; Targeting mitochondrial bioenergetics for Alzheimer's prevention and treatment. Curr Pharm Des. 17 :3474–3479. [PubMed: 21902662]

Yao J, et al. 2009; Mitochondrial bioenergetic deficit precedes Alzheimer's pathology in female mouse model of Alzheimer's disease. Proc Natl Acad Sci U S A. 106 :14670–14675. [PubMed: 19667196]

Ye X, et al. 2012; The early events of Alzheimer's disease pathology: from mitochondrial dysfunction to BDNF axonal transport deficits. Neurobiol Aging. 33 (1122) :e1–10. [PubMed: 22244089]

Yu Q, et al. 2016; Antioxidants rescue mitochondrial transport in differentiated Alzheimer's disease transmitochondrial cybrid cells. J Alzheimers Dis. 54 :679–690. [PubMed: 27567872]

Zhang, L, Trushina, E. Respirometry in neurons. In: Strack, S, Usachev, Y, editors. Techniques to Investigate Mitochondrial Function in Neurons. Springer Nature; 2017. 95–113.

Zhang L, et al. 2015; Modulation of mitochondrial complexIactivity averts cognitive decline in multiple animal models of familial Alzheimer's disease. EBioMedicine. 2 :294–305. [PubMed: 26086035]

Zhang H, et al. 2016a; Geniposide alleviates amyloid-induced synaptic injury by protecting axonal mitochondrial trafficking. Front Cell Neurosci. 10 :309. [PubMed: 28179878]

Zhang L, et al. 2016b; Altered brain energetics induces mitochondrial fission arrest in Alzheimer's disease. Sci Rep. 6 :18725. [PubMed: 26729583]

Zheng X, et al. 2015; Amyloid beta-protein assembly: differential effects of the protective A2T mutation and recessive A2V familial Alzheimer's disease mutation. ACS Chem Neurosci. 6 :1732–1740. [PubMed: 26244608]
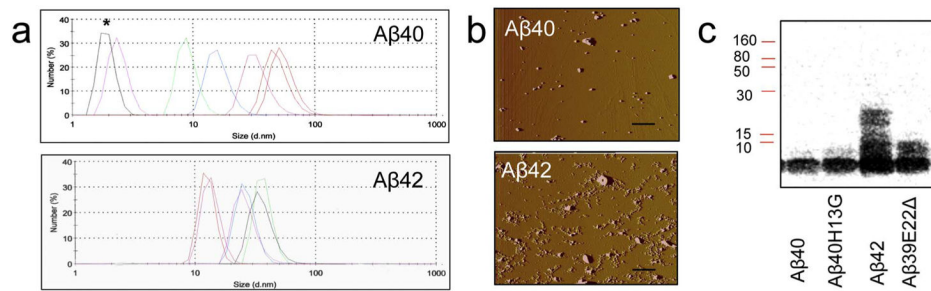
Fig. 1.
Characterization of soluble Aβ40 and Aβ42 species in the solution. (**a**) Dynamic light scattering analysis of particle size distribution in the solutions of Aβ40 and Aβ42 peptides prepared using NH_4OH. Changes in the composition of peptides was observed immediately after the preparation and for the next 30 min; data was collected every 5 min. *, Aβ monomers. (**b**) AFM examination of Aβ40 and Aβ42 peptides (0.1 μM) prepared using NH_4OH and diluted to the final concentration in sodium phosphate buffer. Samples were examined immediately after preparation. Deflection images were collected by raster scanning across a 10 μm^2 area at 1024 samples (pixels) per line at a rate of 3.70 Hz. Scale bar, 1 μm. (**c**) Western blot analysis of Aβ peptides prepared in NH_4OH using specific monoclonal antibody 6E10 against Aβ 1-17.
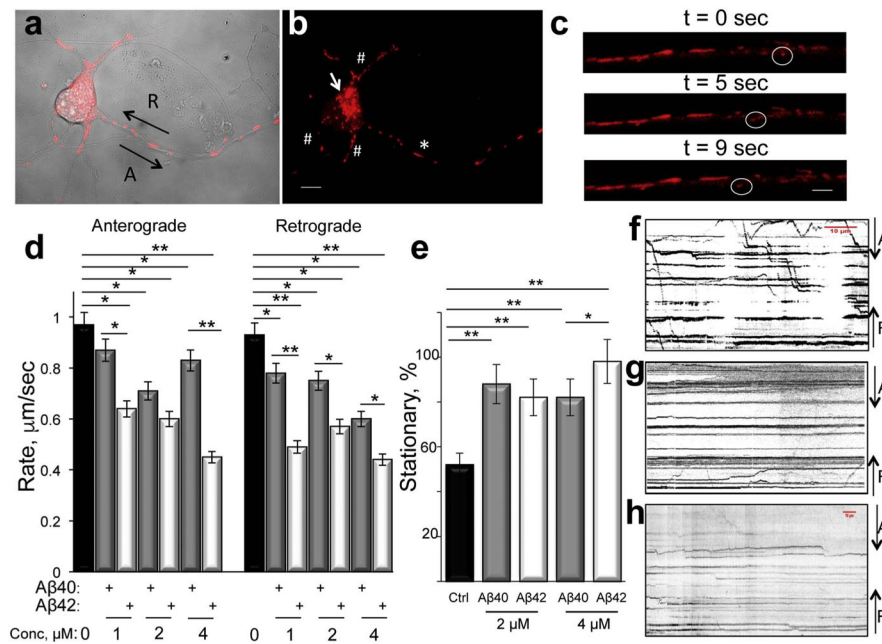
Fig. 2.
Soluble Aβ42 peptides inhibit axonal trafficking of mitochondria to the greater extent than Aβ40 peptides. (**a**) Primary cortical neuron (E17) 7 days in culture treated with TMRM and imaged using confocal microscopy. Axon could be identified as the longest process where mitochondria (red) are moving in anterograde (A) or retrograde (R) direction. (**b**) Individual mitochondria visualized in the same primary neuron as in (**a**) using TMRM in axon (asterisk), dendrites (#), and soma (arrow). Scale bar, 5 μm. (**c**) Time-laps visualization of a mitochondrion (in circle) moving in anterograde direction along the axon in live primary neuron. Scale bar, 1 μm. (**d**) Rates of mitochondrial trafficking in anterograde and retrograde directions is inhibited in live embryonic (E17) primary cortical neurons treated with different concentrations of Aβ40 (grey bars) and Aβ42 (white bars) compared to untreated neurons (black bars). *, $p < 0.01$; **, $p < 0.001$. Analysis was done in three independent cultures; 30 to 57 individual organelles from 15 to 20 neurons were examined. Total fraction of moving mitochondria was ~50% in control neurons; and 10–20% in neurons treated with Aβ40 and Aβ42 peptides. (**e**) Treatment with 2 μM of Aβ40 and Aβ42 peptides resulted in similar increase in stationary mitochondria compared to untreated control neurons. At 4 μM, an increase in stationary mitochondria was particularly evident in neurons treated with Aβ42 peptide. *, $p < 0.01$; **, $p < 0.001$. (**f, g, h**) Aβ40 and Aβ42 treatment significantly inhibits axonal trafficking of mitochondria in neurons. Kymographs generated from the time-lapse movies represent an overview of mitochondrial dynamics over 10 min of observation in (**f**) vehicle - treated, (**g**) Aβ40 – treated, and (**h**) Aβ42 – treated neurons. Horizontal lines indicate stationary mitochondria while diagonal lines represent mitochondria moving in anterograde (A) or retrograde (R) directions.
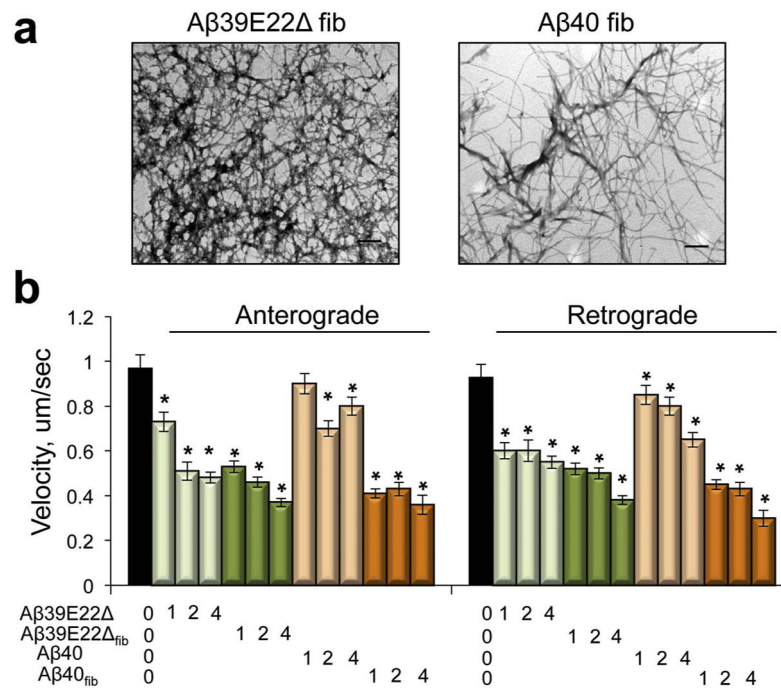
Fig. 3.

Aβ Fibrils affect mitochondrial trafficking to a greater extent than soluble Aβ peptides. (**a**) TEM of Aβ40 and Aβ39E22∆ fibrils 7 days after preparation. Concentration of all peptides is 100 μM. Scale bar, 200 nm. (**b**) Rates of mitochondrial trafficking in live embryonic (E17) cortical neurons treated with Aβ40 and Aβ39E22∆ peptides prepared using NH_4OH or Aβ40 and Aβ39E22∆ fibrils (fib). Concentrations of peptides are in μM. *, $p < 0.01$ (*t*-test compared to untreated neurons). At least 15 neurons from 3 independent cultures were analyzed for each experiment. 35–70 individual organelles were taken into the analysis for each condition.
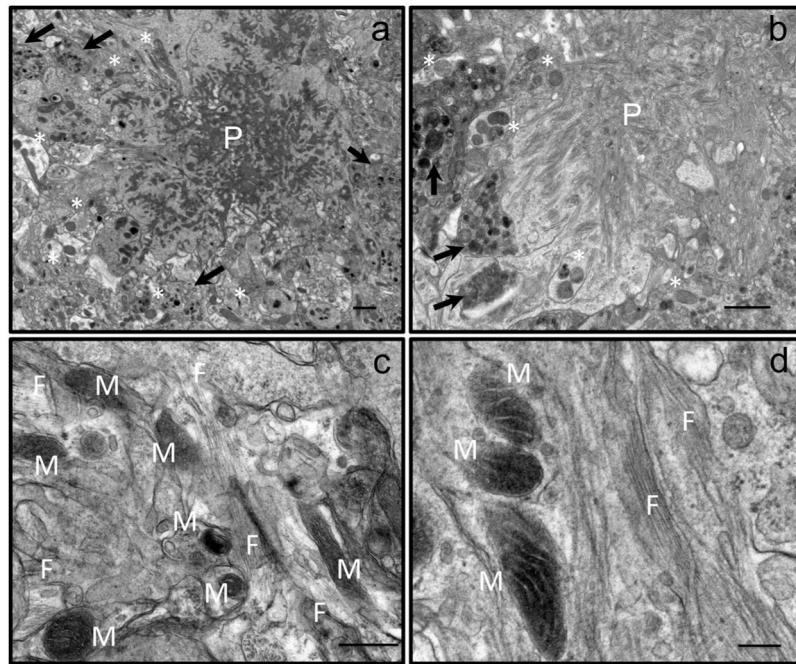
Fig. 4.

Aβ Fibrils have a direct contact with neurites containing mitochondria in the hippocampal brain tissue of young and old APP/PS1 mice. (**a, b**) Low magnification EM micrograph showing an amyloid plaque (P) surrounded by dystrophic neurites (arrows) in the hippocampal CA1 region of a 6-months-old (**a**) and 22-months old (**b**) APP/PS1 mice. Dystrophic neurites are filled with vesicles that contain electron-dense material. Asterisks denote neuritis with mitochondria. (**a**) Scale bar, 1 μm. (**b**) Scale bar, 2 μm. (**c, d**) High magnification EM micrographs of amyloid fibrils (F) located in close proximity to neurites containing mitochondria (M) in the brain tissue of young (**c**) and old (**d**) APP/PS1 mice. Individual fibrils (F) could be clearly seen. Scale bars: (**c**) 50 nm; (**d**) 200 nm.
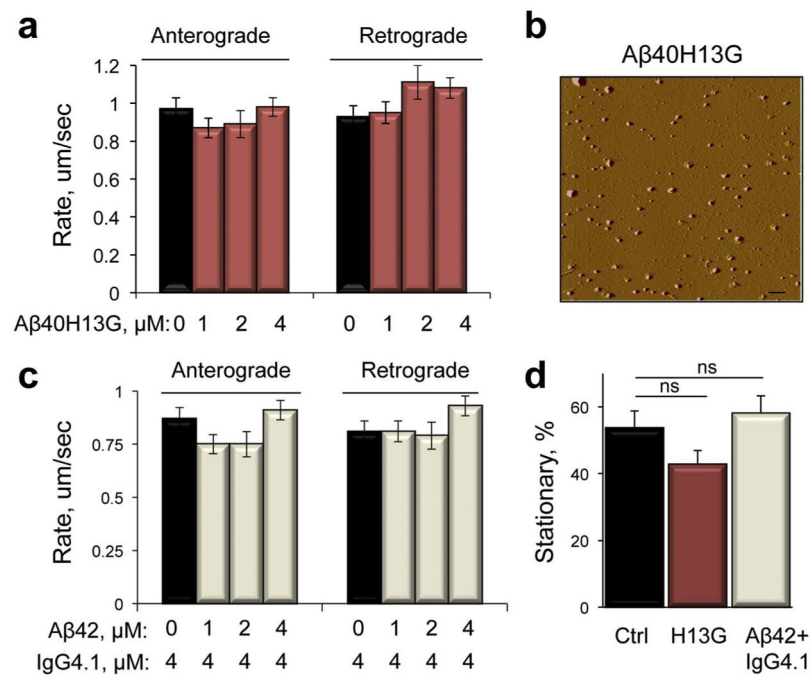
Fig. 5.
Reduced plasma membrane binding of Aβ peptides or capture with Aβ-specific antibody rescues trafficking phenotype. (**a**) Aβ40H13G peptide with reduced binding to the plasma membrane does not affect axonal trafficking of mitochondria in embryonic (E17) cortical neurons. Black bars – untreated neurons; red bars – neurons treated with different doses of Aβ40H13G. (**b**) AFM of Aβ40H13G peptide (0.1 μM) immediately after preparation using NH_4OH. Scale bar, 1 μm. (**c**) Rates of mitochondrial trafficking in embryonic neurons pre-treated with specific anti- Aβ IgG4.1 antibody and post-treated with different doses of Aβ42. Black bars –neurons treated with IgG4.1 alone; grey bars – neurons pretreated with IgG4.1 and post-treated with Aβ42. (**d**) Analysis of mitochondria motility indicates no increase in stationary mitochondria in neurons treated with Aβ40H13G (H13G) or Aβ42 after pretreatment with IgG4.1 antibody. ns, not significant (*t*-test compared to untreated neurons). At least 15 neurons from 3 independent cultures were analyzed for each experiment. 35–70 individual organelles were taken into the analysis for each condition.
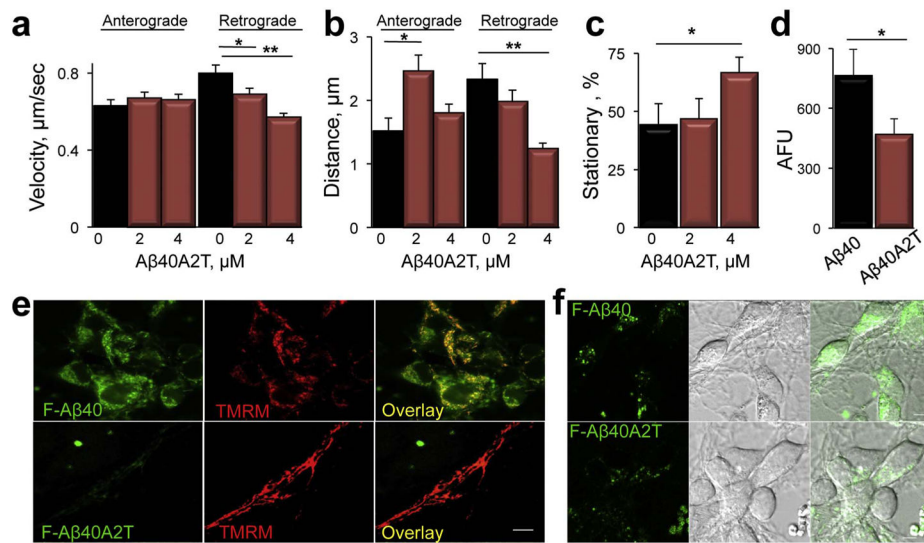
Fig. 6.

Aβ40A2T peptide with Icelandic mutation differentially affects mitochondrial trafficking and has reduced rate of internalization in neurons compared to Aβ40. (**a**) Treatment with Aβ40A2T inhibits retrograde transport of mitochondria in a dose-dependent manner. *, $p < 0.05$; **, $p < 0.01$. (**b**) Mitochondria in Aβ40A2T-treated neurons travel shorter distances in retrograde direction and increased distances in anterograde direction compared to untreated cells. (**c**) Treatment with Aβ40A2T increases the amount of stationary organelles. *, $p < 0.05$. (**d**) Quantification of internalization experiments with fluorescein-labeled F-Aβ40A2T and F-Aβ40 presented in (**e** and **f**). *, $p < 0.05$. (**e**, **f**) Internalization of fluorescein-labeled F-Aβ40A2T (4 μM) is reduced in primary neurons compared to F-Aβ40. 40–60 cells from two independent experiments were taken into the analysis. AFU, arbitrary fluorescence units. *, $p < 0.05$. Confocal images were taken 10 min after the addition of Aβ peptides to cells. Internalized F- Aβ40 (green) colocalized with mitochondria visualized using TMRM (**e**, red). DIC images together with fluorescence images are provided in (**f**). Images were acquired using LSM 780 laser scanning microscope (Carl Zeiss) with 100× oil DIC (1.4 n.a.) lens. Scale bar, 5 μm.
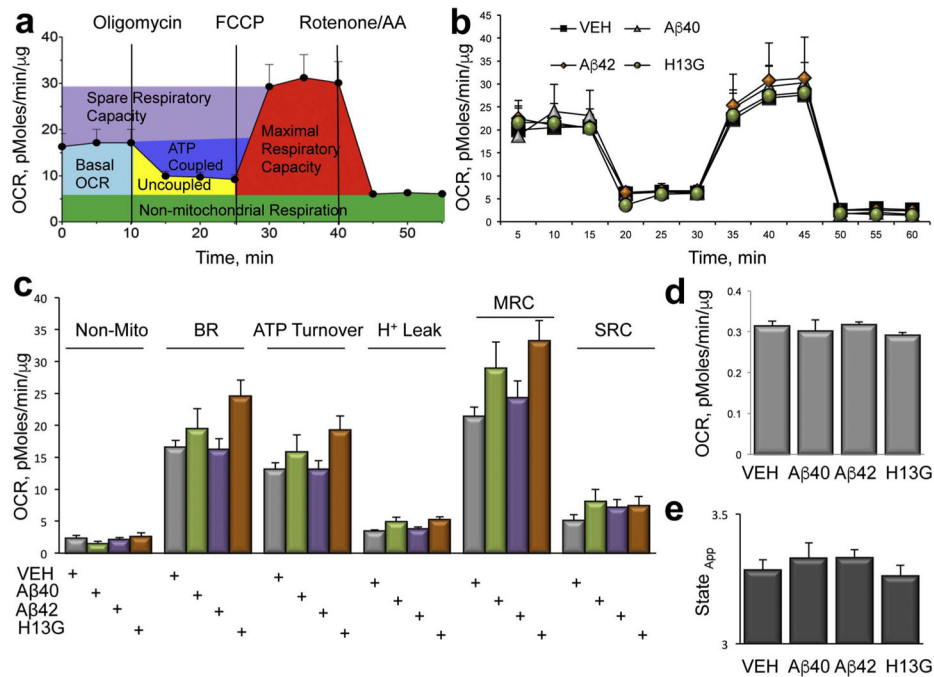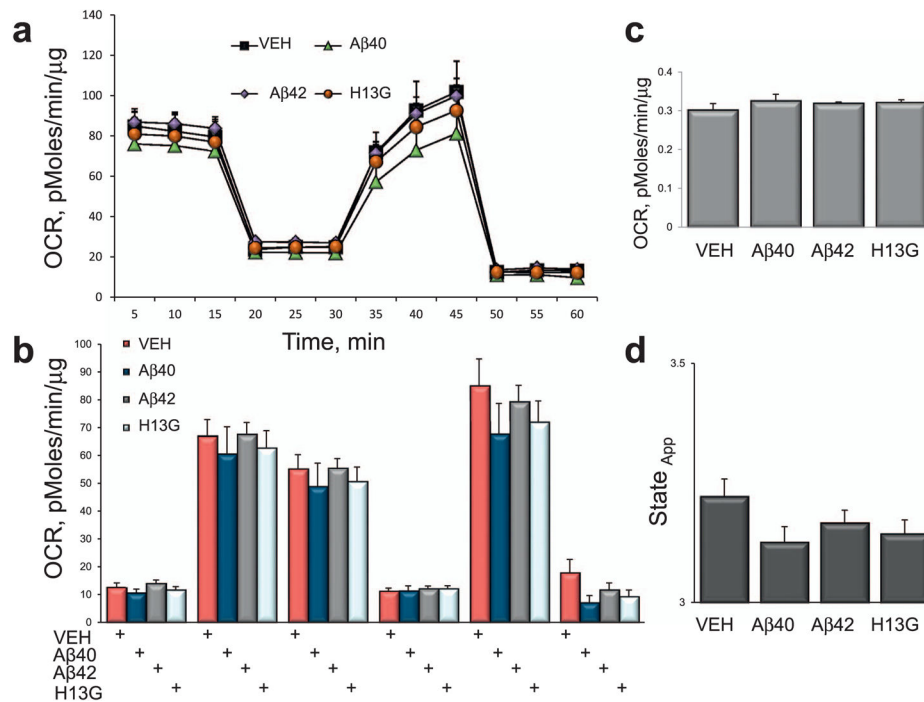
Fig. 7.
Inhibition of axonal trafficking in neurons treated with soluble Aβ peptides does not affect mitochondrial function. (**a**) Parameters of mitochondrial respiration acquired in intact live primary neurons treated with different Aβ peptides using a Seahorse XF24 Extracellular Flux Analyzer. Measurements of oxygen consumption rates (OCR) in the absence or presence of specific mitochondrial toxins allows to estimate the following parameters: basal OCR (light blue); ATP-coupled respiration (dark blue) and proton leak (Uncoupled, yellow) after the addition of 1 μg/ml oligomycin; maximal (MRC, red) and spare (SRC, purple) respiratory capacity after an addition of 0.75 μM FCCP. The contribution of non-mitochondrial (green) respiration to basal OCR is determined as the activity remaining after the inhibition of complexes I and III with 0.75 μM rotenone and 0.75 μM antimycin A (AA). (**b**) Treatment of intact primary neurons with 2 μM Aβ42 (diamonds), 2 μM Aβ40H13G (circles) or 2 μM Aβ40 (triangles) did not affect mitochondrial energetics compared to neurons treated with vehicle (squares). Each data point is compiled from 6 to 8 individual wells from 3 independent experiments. (**c**) Analysis of the experiments conducted in (**b**). (**d**) Quantification of mitochondria coupling efficiency. (**e**) Estimation of mitochondria state apparent.

Fig. 8.
Inhibition of axonal trafficking in neurons treated with 7-days Aβ fibrils does not affect mitochondrial function. (**a**) Treatment of intact primary neurons with 2 μM Aβ42 (diamonds), 2 μM Aβ40 (triangles) or 2 μM Aβ40H13G (circles) did not affect mitochondrial energetics compared to neurons treated with vehicle (squares). Each data point is compiled from 6 to 8 individual wells from 3 independent experiments. (b) Parameters of mitochondrial respiration acquired in intact primary neurons treated with different Aβ fibrils using a Seahorse XF24 Extracellular Flux Analyzer. Measurements of oxygen consumption rates (OCR) in the absence or presence of specific mitochondrial toxins allows to estimate the following parameters: basal OCR (light blue); ATP-coupled respiration (dark blue) and proton leak (Uncoupled, yellow) after the addition of 1 μg/ml oligomycin; maximal (MRC, red) and spare (SRC, purple) respiratory capacity after an addition of 0.75 μM FCCP. The contribution of non-mitochondrial (green) respiration to basal OCR is determined as the activity remaining after the inhibition of complexes I and III with 0.75 μM rotenone and 0.75 μM antimycin A (AA). (**c**) Quantification of mitochondria coupling efficiency. (**d**) Estimation of mitochondria state apparent.

Table 1

Peptides used in the study.

Peptide	Sequence	Notes	References
Aβ40	DAEFRHDSGYEVHHQKLVFFAEDVGSNKGAIIGLMVGGVV	Most common peptide that forms soluble and fibrillar structures	(Hellstrand et al., 2010)
Aβ42	DAEFRHDSGYEVHHQKLVFFAEDVGSNKGAIIGLMVGGVVIA	Soluble up to 0.1–0.2 μM; at higher concentrations aggregates into well-ordered μ-sheet- rich fibrillar structures	(Hellstrand et al., 2010)
Aβ39E22	DAEFRHDSGYEVHHQKLVFFADVGSNKGAIIGLMVGGVV	Accelerated aggregation in solution	(Kassler et al., 2010; Nishitsuji et al., 2009; Ovchinnikova et al., 2011; Tomiyama et al., 2008)
Aβ40H13G	DAEFRHDSGYEVGHQKLVFFAEDVGSNKGAIIGLMVGGVV	Reduced plasma membrane binding	(Poduslo et al., 2010)
Aβ40A2T	DTEFRHDSGYEVHHQKLVFFAEDVGSNKGAIIGLMVGGVV	Proposed protective effect of this mutation is associated with reduced BACE1-mediated APP cleavage and low levels of Aβ production	(Jonsson et al., 2012; Maloney et al., 2014)